ACIBADEM MEHMET ALI AYDINLAR UNIVERSITY
INSTITUTE OF HEALTH SCIENCES

# APPLICATION OF QUARTZ CRYSTAL MICROBALANCE AS AN ALTERNATIVE METHOD FOR ASSESSING BLOOD COAGULATION TIME AND VISCOELASTIC PROPERTIES OF FIBRIN FORMATION

FATIMA ŞEYMA ELBEYOĞLU

M.Sc. THESIS

DEPARTMENT OF BIOPHYSICS

SUPERVISOR
Assoc. Prof. Evren KILINÇ

SECONDARY SUPERVISOR
Assist. Prof. Ceyhun Ekrem KIRIMLI

ISTANBUL-2024

ACIBADEM MEHMET ALI AYDINLAR UNIVERSITY
INSTITUTE OF HEALTH SCIENCES

# APPLICATION OF QUARTZ CRYSTAL MICROBALANCE AS AN ALTERNATIVE METHOD FOR ASSESSING BLOOD COAGULATION TIME AND VISCOELASTIC PROPERTIES OF FIBRIN FORMATION

FATIMA ŞEYMA ELBEYOĞLU

M.Sc. THESIS

DEPARTMENT OF BIOPHYSICS

SUPERVISOR
Assoc. Prof. Evren KILINÇ

SECONDARY SUPERVISOR
Assist. Prof. Ceyhun Ekrem KIRIMLI

ISTANBUL-2024

## DECLARATION

I hereby declare that; this thesis has been written by me based on the data obtained in line with the scientific rules and ethical principles of responsible conduct of research. All information, data, comments, analyses have been collected and processed through scientific, academic writing style, and literature used have been duly shown by giving reference to the original sources in accordance with the publication ethics. I also announce and emphasize that I have not violated any rules secured by patent and copyrights whilst the conduct and writing of this research.

25/11/2024
Fatıma Şeyma Elbeyoğlu

## PREFACE AND ACKNOWLEDGEMENT

I express my deepest gratitude to my esteemed supervisors, Assoc. Prof. Evren KILINÇ and Assist. Prof. Ceyhun Ekrem KIRIMLI, for their invaluable guidance, unwavering support, and constant encouragement throughout my master's thesis research. Their expertise, insightful feedback, and commitment to my academic success have been instrumental in shaping the outcome of this thesis. I am profoundly grateful for the countless hours they have dedicated to reviewing my work, providing constructive criticism, and challenging me to think critically and analytically. Assoc. Prof. Evren KILINÇ's deep understanding of the subject matter and his ability to offer innovative perspectives have been a true source of inspiration, pushing me to explore new avenues of research and expand the boundaries of my knowledge. Assist. Prof. Ceyhun Ekrem KIRIMLI's meticulous attention to detail, practical suggestions, and willingness to engage in thought-provoking discussions have been crucial in refining and polishing my work, ensuring it meets the highest academic standards. I am incredibly fortunate to have had the opportunity to work under their guidance and mentorship, and I will forever be indebted to them for their invaluable contributions to my academic journey. I also want to thank my friends and family for their unwavering support, understanding, and encouragement throughout this challenging yet rewarding process. Without their constant belief in me and their willingness to offer a listening ear during moments of doubt, completing of this thesis would not have been possible.

I thank The Scientific and Technological Research Council of Türkiye (TÜBİTAK) Directorate of Science Fellowships and Grant Programmes (BİDEB) 2210-A National MSc/MA Scholarship Program for supporting my finances during my academic journey.

# TABLE OF CONTENTS

## ABBREVIATIONS AND SYMBOLS

| | |
|---|---|
| **aPTT** | Activated Partial Thromboplastin Time |
| **Au** | Gold |
| **$CaCl_2$** | Calcium Chloride |
| **df** | Degrees of Freedom |
| **$\Delta f$** | Frequency Change |
| **Hz** | Hertz |
| **LDPE** | Low-Density Polyethylene |
| **$\Delta m$** | Mass Change |
| **PMMA** | Polymethyl Methacrylate |
| **PPP** | Platelet Poor Plasma |
| **PTT** | Prothrombin Time |
| **$\mu$** | Shear Modulus |
| **SEM** | Scanning Electron Microscope |
| **$\eta$** | Shear Viscosity |
| **Ti** | Titanium |
| **QCM** | Quartz Crystal Microbalance |

# LIST OF FIGURES

# LIST OF TABLES

# ABSTRACT

**Application of Quartz Crystal Microbalance as an Alternative Method for Assessing Blood Coagulation Time and Viscoelastic Properties of Fibrin Formation**

This thesis investigates the use of Quartz Crystal Microbalance (QCM) technology as an alternative to conventional activated partial thromboplastin time (aPTT) tests for real-time monitoring of blood clotting dynamics in platelet-poor plasma (PPP). SEM analysis of QCM sensor coatings revealed that polymethyl methacrylate (PMMA) coatings provide more consistent thickness and stability compared to low-density polyethylene (LDPE), which exhibited a non-homogeneous structure. This finding emphasizes that PMMA coatings are more suitable for reliable QCM measurements in liquid environments. In the study, clots were formed in PPP samples using both undiluted and diluted aPTT reagents across different harmonic frequencies, and critical parameters were derived through frequency curve analysis. Clots formed with diluted aPTT reagents showed a prolonged clotting time, reduced maximum clot firmness, and a decreased area under the curve, resulting in compromised clot stability. The results indicate that higher frequencies, particularly 30 and 50 MHz, provide greater sensitivity and better reflect differences in reagent concentration. Additionally, using a modified 3-layer Kelvin-Voigt model, parameters revealing the viscoelastic properties of clots such as clot thickness, shear modulus, and shear viscosity were calculated. It was observed that reagent dilution significantly reduced the shear modulus, indicating a decrease in clot stiffness and mechanical integrity. Although clot thickness and shear viscosity were largely unaffected by reagent dilution, the reduction in shear modulus suggests a weaker fibrin network with lower resistance to deformation. In conclusion, QCM emerges as a powerful alternative method for precise and real-time monitoring of the clot formation process through multi-harmonic analysis and advanced viscoelastic modeling.



**Keywords:** Blood clotting dynamics, Activated partial thromboplastin time, Quartz Crystal Microbalance, Viscoelasticity, Multi-harmonic frequencies

# ÖZET

**Kan Pıhtılaşma zamanı ve Fibrin Oluşumunun Viskoelastik Özelliklerinin Değerlendirilmesinde Alternatif Bir Yöntem Olarak Kuartz Kristal Mikrobalans (QCM) Kullanımı**

Bu tez, plateletten fakir plazmada (PFP) kan pıhtılaşma dinamiklerinin gerçek zamanlı izlenmesi için geleneksel aktive parsiyel tromboplastin zamanı (aPTT) testine alternatif olarak Kuvars Kristal Mikrobalans (QCM) teknolojisinin kullanımını araştırmaktadır. QCM sensör kaplamalarının SEM analizi, polimetil metakrilat (PMMA) kaplamaların düşük yoğunluklu polietilen (LDPE) kaplamalara göre daha tutarlı kalınlık ve stabilite sunduğunu, LDPE'nin ise homojen olmayan bir yapı sergilediğini göstermiştir. Bu çalışmada farklı harmonik frekanslar altında, seyreltilmemiş ve seyreltilmiş aPTT reaktifi ile PFP örneklerinde pıhtılar oluşturulmuş ve frekans eğrileri analiz edilerek önemli parametreler türetilmiştir. Seyreltilmiş aPTT reaktifi ile oluşturulan pıhtılarda, pıhtılaşma süresi uzamış, maksimum pıhtı sertliği ve eğri altında kalan alan değerleri azalarak pıhtı stabilitesi olumsuz etkilenmiştir. Sonuçlar, yüksek frekansların daha yüksek hassasiyet sunduğunu ve reaktif yoğunluğundaki farklılıkları daha iyi yansıttığını göstermektedir. Ek olarak, modifiye edilmiş 3-katmanlı Kelvin-Voigt modeli kullanarak pıhtı kalınlığı, kayma modülü, viskozite gibi pıhtıların viskoelastik özelliklerini ortaya koyan parametreler hesaplanmıştır. Reaktif seyreltmenin, pıhtının sertliğinde ve mekanik bütünlüğünde azalmayı işaret eden kayma modülünü önemli ölçüde azalttığı gözlenmiştir. Pıhtı kalınlığı ve kayma viskozitesi reaktif seyreltilmesinden büyük ölçüde etkilenmemiş olsa da kayma modülündeki azalma, daha zayıf ve deformasyona karşı direnci düşük bir fibrin ağına işaret etmektedir. Sonuç olarak, QCM, çok harmonikli analiz ve gelişmiş viskoelastik modelleme ile pıhtı oluşum sürecini hassas ve gerçek zamanlı olarak izlemek için güçlü bir alternatif yöntem olarak öne çıkmaktadır.

**Anahtar Sözcükler:** Kan pıhtılaşma dinamikleri, Aktive parsiyel tromboplastin zamanı, Kuvars Kristal Mikrobalans, Viskoelastisite, Çoklu-harmonik frekanslar

# 1 INTRODUCTION AND AIM

## 1.1 Importance of Blood Coagulation Monitoring

Blood coagulation is a crucial physiological process that ensures hemostasis protecting the body from excessive blood loss. This process involves a complex cascade of reactions that result in clot formation, making accurate monitoring essential in diagnosing and managing bleeding disorders such as hemophilia, thrombocytopenia, and thrombotic conditions (1). Early detection and monitoring are vital, particularly in high-risk populations, where early intervention can significantly improve clinical outcomes. Traditional coagulation tests, including Prothrombin Time (PT) and activated Partial Thromboplastin Time (aPTT), remain as gold standard due to their foundational diagnostic role in clinical practice. Despite their prevalence, these tests are limited in their ability to capture detailed coagulation dynamics, presenting challenges in precise diagnostic and monitoring capabilities.

Blood coagulation disorders constitute a significant global health burden, affecting millions worldwide. The conditions often require lifelong management, and detailed monitoring is essential for improving patient care. Inaccurate or delayed detection of coagulation abnormalities can lead to serious outcomes, particularly in individuals undergoing anticoagulant therapy. Thus, there is a critical demand for monitoring methods that are both sensitive and capable of real-time assessment, providing clinicians with the necessary tools for effective diagnosis and treatment. The importance of continuous, precise coagulation monitoring becomes even more pronounced in intensive care, where rapid changes in a patient's coagulation status require immediate and accurate intervention.

## 1.2 Limitations of Conventional Coagulation Tests

Conventional coagulation tests are inherently limited by their methodological and technical constraints, which often compromise their diagnostic precision. Traditional PT and aPTT tests, while useful, are generally not sensitive enough to detect minor

abnormalities in coagulation, particularly during early-stage clot formation (1). This insensitivity to initial clotting events may lead to diagnostic delays, potentially overlooking subtle coagulation disorders that could indicate an underlying pathology. Furthermore, many of these assays require substantial blood volumes, which poses a particular challenge in pediatric and neonatal care, where conserving blood samples is essential (2). The inability of conventional tests to perform with smaller volumes often renders them impractical in such settings, limiting the options available for young patients.

The reliance on spectrophotometric methods in traditional coagulation tests presents another limitation, as these methods are generally unsuitable for whole-blood samples. Optical interference from red blood cells can distort results, thereby reducing the accuracy of spectrophotometric assessments in whole-blood analysis (3). As a result, these methods typically require extensive sample processing to remove cellular components, which introduces additional preparation time and potentially delays diagnostic feedback. The intermittent nature of these tests, which typically provide only endpoint measurements, further limits their utility. These kinds of measurements do not capture real-time data on clot formation and stabilization, thereby offering an incomplete picture of the coagulation process (4). Real-time monitoring is essential in critical care scenarios, where factors like temperature and shear stress affect clot formation. Traditional tests, however, cannot simulate physiological conditions accurately, leading to potential discrepancies between laboratory findings and clinical outcomes (5).

### 1.3 Aim of the Study

This study seeks to address the limitations of traditional coagulation monitoring methods by exploring the application of Quartz Crystal Microbalance (QCM) technology in blood coagulation monitoring, specifically through aPTT measurements. QCM technology provides a novel approach due to its high sensitivity and continuous data acquisition capabilities, enabling it to capture subtle shifts in clot formation that traditional methods might miss. By measuring frequency shifts and

resonant behavior in response to clot formation, QCM facilitates the real-time tracking of coagulation dynamics, particularly in the early and progressive stages of clot development. This real-time monitoring capability is essential for understanding how physiological factors impact coagulation, offering a detailed perspective that endpoint-based methods cannot achieve.

The novelty of this study is further underscored by its focus on viscoelastic properties of coagulating blood samples, which QCM is uniquely equipped to assess. Through the analysis of frequency shifts and multi-harmonic responses, QCM technology can provide insight into the clot's mechanical properties as they develop, enabling a more comprehensive examination of the coagulation process. This study's findings aim to expand the understanding of clot formation dynamics and offer a new approach for monitoring coagulation, particularly in clinical settings where sensitivity and real-time data are crucial.

One of the innovative aspects of this study is the utilization of specialized coatings on QCM sensors to enhance measurement accuracy and sensitivity. An initial assessment of Low-Density Polyethylene (LDPE) as a coating material revealed several limitations, such as stiffness and challenges in achieving a uniform coating over the QCM surface. Consequently, Polymethyl Methacrylate (PMMA) was selected for its compatibility with the QCM system and its favorable mechanical properties, which facilitate consistent interaction with blood components during the coagulation process. The PMMA coating enables more precise measurement of frequency shifts and enhances the sensor's sensitivity to viscoelastic changes during clot formation.

Using PMMA-coated QCM sensors this study aims to capture multi-harmonic responses in coagulating blood, a methodological advancement that allows for a thorough analysis of the clot's mechanical properties. This approach addresses key limitations in traditional methods by offering a more sensitive and adaptable platform for coagulation monitoring. By examining the viscoelastic properties and clot stability through continuous monitoring, this study aims to provide a novel perspective on blood coagulation dynamics.

In addition to addressing limitations in existing methods, this study aims to evaluate the potential of QCM as a clinically viable diagnostic tool. Conventional spectrophotometric methods are often unsuitable in settings where optical interference is present, particularly in whole-blood analysis. QCM's ability to operate effectively in optically interfered environments makes it a promising alternative for coagulation testing without the need for extensive sample processing (6, 7). Given its capability for real-time monitoring, QCM has the potential to significantly enhance diagnostic precision in coagulation measurements, providing clinicians with timely information on clot formation dynamics.

This research contributes to the development of advanced diagnostic tools by highlighting QCM as a potential alternative for traditional coagulation tests, particularly in critical care and surgical settings where accurate monitoring is essential. By exploring the feasibility of integrating QCM technology into clinical workflows, this study highlights the potential benefits of QCM-based diagnostics in improving patient outcomes through more sensitive and timely coagulation assessments.

# 2 BACKGROUND

## 2.1 Blood Coagulation

Blood coagulation is a complex process that plays an important role in maintaining hemostasis and preventing excessive bleeding. It was described by group of scientists in 1960's as two theories called 'cascade' and 'waterfall' (1). The term hemostasis is derived from "hem-" meaning "blood" and "-stasis" meaning "to stop" Therefore, hemostasis means stopping bleeding (1). There are two stages to hemostasis: First, primary hemostasis occurs to form 'platelet plug'. This process is caused by complex interactions of vessel walls, platelets and adhesive proteins (8). The coagulation cascade is then activated to stabilize the clot and stop blood flow, providing time for the necessary repairs to be done. The process of the coagulation cascade involves the initiation of a sequence of clotting factors, which are proteins involved in the process of blood clotting and this process is called secondary hemostasis (1). Within the cascade, there are clotting factors which are responsible for clot formation. Each of these clotting factors functions as a serine protease, which is an enzymatic agent that facilitates the acceleration of the degradation process of another protein. In their nascent state, the clotting factors exist as zymogens, displaying an inactive behavior. When they interact with their respective glycoprotein co-factor, the clotting factor undergoes activation, consequently enabling it to accelerate the upcoming biochemical reaction (9). The activated clotting factor is indicated by adding an "a" subsequent to its corresponding Roman numeral. Coagulation cascade consists of two pathways called intrinsic and extrinsic pathway leading to a common pathway to form a clot. Intrinsic pathway is also called contact activation pathway, and it is a complex cascade that is essential for normal clot formation after vascular injury. This process involves a series of proteins, including factor XII (FXII), high-molecular-weight kininogen, prekallikrein, and factor XI. Intrinsic pathway is triggered with activation of FXII upon contacting negatively charged surfaces, such as collagen secreted from injury site. Then FXI further activates FIX, and it acts with the cofactor FVIII in succession, leading to the activation of FX. The intrinsic pathway is initiated slower when compared to the extrinsic pathway and is usually triggered simultaneously during

tissue injury. On the other hand, extrinsic pathway is initiated by external trauma or blood leak. It is triggered by tissue factor binds to one of coagulation factors, FVII, which then becomes activated to FVIIa. The tissue factor/factor VIIa complex then activates FX, skipping the earlier steps of the intrinsic pathway, which is why the extrinsic pathway is also known as the rapid or tissue factor pathway (10). Both extrinsic and intrinsic pathways converge at FX, which, once activated to FXa, combines with factor V in the presence of calcium ions and phospholipids to form the prothrombinase complex. This complex then catalyzes the conversion of prothrombin into thrombin. Thrombin then operates multiple functions: it converts fibrinogen to fibrin to form the structural basis of a clot, it activates FXIII which crosslinks the fibrin clot, and it also feeds back to activate factors V, VIII, and XI within the intrinsic pathway, accelerating the coagulation process (5).

### 2.1.1 Coagulation tests

The coagulation mechanism is kept under balance, until it is disrupted by pathogenic conditions, genetic factors or when an organism is exposed to chemicals. In clinics, monitoring coagulation is very crucial in terms of patient's health (1). There are diverse methodologies used to monitor secondary hemostasis in terms of detecting coagulopathies and following the anticoagulant treatments (11). Clot-based tests are used to mimic two pathways of coagulation: intrinsic and extrinsic pathways. These techniques aim to measure the time takes blood to clot and are useful for screening patients with possible bleeding disorders by mainly measuring fibrin formation (1). Most common clot-based tests are PT and aPTT. The PT test is a measurement of the time it takes for plasma to clot after substances are added to initiate the clotting process (1,11). This test is used to assess the integrity of the extrinsic and common pathways of the coagulation cascade and is primarily employed to monitor the effectiveness of anticoagulant therapy, such as warfarin, and to investigate bleeding or clotting disorders (11). The results of the PT test are typically reported as an international normalized ratio (INR), which standardizes the PT results to account for variations in reagents and instruments. On the other hand, the aPTT assay is used to evaluate the intrinsic and common pathways of the coagulation cascade. It is commonly employed

to monitor patients receiving heparin therapy and to investigate unexplained bleeding or clotting. Similar to the PT test, blood is collected into a tube containing an anticoagulant, and the plasma is separated from the blood cells for the aPTT assay. The results of the aPTT assay are reported as the time in seconds that it takes for the plasma to clot (2,12).

Both the PT test and aPTT assays are valuable tools for assessing the coagulation status of patients and are essential in the diagnosis and management of bleeding and clotting disorders. Other than PT and aPTT, Fibrinogen assay and D-Dimer tests are also performed to investigate blood clots (11). Fibrinogen assay measures the level of fibrinogen. It is used to diagnose and monitor conditions associated with abnormal fibrinogen levels, such as liver disease, disseminated intravascular coagulation, and certain inherited coagulation disorders. On the other hand, D-Dimer tests is for detection of the small protein fragment called D-dimer, which presents when clot dissolves. D-dimer test is used to diagnose or rule out blood clots, such as pulmonary embolism and deep vein thrombosis (13). There are also optic based clotting tests, which are used for identification of clot formation visually. Their working principle is based on monitoring increased scattered light and decreased transmitted light. When fibrin strands form within the test cuvette, it leads to a rise in cloudiness of the plasma sample, which also means reduced light transmission. Decrease in light transmission is interpreted as a change in light absorption per minute (ΔOD/min). These systems can plot clotting as waveforms, providing insights into the dynamics of clot formation. Chromogenic assays are a type of coagulation test that play a crucial role in measuring the activity of specific clotting factors in the blood. These assays depend on chromogenic substrates, which are cleaved by the target clotting factor, then colored product is produced and can be measured spectrophotometrically (14). Compared to clot-based tests, chromogenic assays are more specific and accurate as they directly measure the activity of the clotting factor of interest (14). These assays are typically carried out using automated machines, which are capable of accurately detecting and measuring the colored product generated by the cleavage of the chromogenic substrate. Overall, chromogenic assays offer a reliable and precise method for evaluating the activity of specific clotting factors in the blood, making them an indispensable tool in

the diagnosis and management of coagulation disorders. Most commonly, the study of coagulation has relied on these various techniques and assays to measure different aspects of the coagulation process. However, traditional clotting assays like PT and aPTT do not provide continuous, real-time data on the dynamics of clot formation and progression, which is crucial in clinical scenarios such as surgeries requiring anticoagulants or in managing coagulation disorders (1). Additionally, these tests often rely on spectrophotometric techniques, which cannot be effectively applied to whole blood due to optical interference from red blood cells or in hemolytic plasma samples. Given these challenges, there is a growing need for alternative methods that allow for more sensitive, continuous, and interference-free monitoring of blood coagulation (1,2).

Recently biosensors have come up as a popular topic due to their real-time application potential and high sensitivity in both clinical and industrial research (4). One of the acoustic wave biosensors, QCM has emerged as a highly valuable alternative for the determination of surface-induced blood coagulation. The QCM is particularly advantageous for monitoring blood coagulation due to its ability to detect the viscoelastic properties and phase transitions of clots. This capability allows for precise observation of the biomechanical changes occurring during coagulation, making QCM a highly effective tool compared to other biosensors. Using QCM technology in the investigation of blood coagulation is a promising research area for biomedical diagnostics. This technology offers a label-free, real-time monitoring of the coagulation cascade, providing a window into the dynamic interplay of clotting factors at the surface level as well as assessing viscosity (15). Unlike optical methods, QCM is unaffected by sample opacity, which allows it to monitor coagulation in whole-blood samples without interference from red blood cells. Measuring coagulation directly in whole blood is particularly valuable as it more accurately represents the physiological state of clot formation. Unlike plasma-based assays, whole blood measurements account for the influence of cellular components like red blood cells and platelets, which play significant roles in clotting dynamics. This approach offers a more comprehensive view of coagulation processes, making it especially useful in clinical settings where real-time, physiologically relevant data are

essential. This provides a major advantage in clinical diagnostics, particularly in scenarios where traditional methods may fail. QCM's ability to continuously track changes in clot formation, alongside its high sensitivity, positions it as a versatile tool for coagulation studies.

## 2.2 Quartz Crystal Microbalance (QCM)

Measurement of weight and mass has been one of the fundamental curiosities and necessities of humanity for a long time. Originating from the simple methods involving balancing weights on a suspended stick that were used, more advanced techniques have since been developed, such as spring expansion measurements and the use of resonators (16). These sophisticated methods are highly accurate and precise, capable of measuring even small masses, with resonators significantly enhancing measurement accuracy, precision, and resolution. Moreover, miniaturized bulk acoustic wave (BAW) resonators enable the creation of high-sensitivity gravimetric sensors, allowing for the measurement of even a few molecules level in laboratory conditions (16). The QCM is a well-established resonator-based mass sensor. It consists of a quartz crystal sandwiched between two metal electrodes (17). QCM measures resonance frequency changes generated by the quartz crystal sensor when covered with a thin film or liquid. A typical QCM setup consists of a quartz crystal sensor, a precision oscillator circuit, and a data acquisition system (18). The crystal sensor surface is coated with the material of interest, and the resulting frequency changes are detected by the oscillator circuit and converted into mass or viscosity measurements (7). The QCM can be covered with different coating materials for detection of specific molecules or materials. When a molecule or assembly binds to the crystal surface, it causes a shift in the resonance frequency of the crystal. This frequency shift can be detected and measured, and it provides information about the mass of the bound molecules or assemblies (7). QCM can be used as a mass sensor and has potential applications in various fields, including materials science, biology, environmental science, and analytical chemistry. The development of portable QCM systems is desired for field-deployable applications and in situ detection. A miniaturized QCM device has been successfully fabricated, showing its potential as a portable biosensor (19).

The history of the QCM dates to the early 1950s when it was first developed as a tool for measuring thin film deposition rates in vacuum systems (17). Since then, it has evolved into a versatile and widely used tool in various research fields such as material science, biology, chemistry, and nanotechnology. In chemistry, the QCM can be used to investigate corrosion processes and oxidation kinetics by monitoring changes in the mass or viscoelastic properties of the electrodeposited films, providing a deeper understanding of these processes as well as in measuring solubility and diffusion (20).

In material science, it is used to study the growth and properties of thin films and coatings. It is also used in the characterization of surface interactions and adsorption processes (7). Moreover, QCM allows to study of chemical reactions occurring on the crystal surface, such as catalytic reactions, surface modification, and molecular binding events, enabling detailed analysis of various chemical processes. In biology, QCM is utilized in studying molecular interactions, and biomolecular interactions, such as antibody-antigen binding, DNA hybridization, cell adhesion, and receptor-ligand interactions on the crystal surface. Ongoing research and technological advancements continue to enhance the performance and broaden the applications of QCM in diverse areas of study (21).

In QCM measurements, while the fundamental frequency is the most used to momonitore mass changes and interactions, higher order harmonics can also be utilized for more advanced analyses (7). Analyzing the response of different harmonics helps to gain more information about the elasticity, viscosity, and mechanical properties of the deposited films, contributing to material science and surface engineering. Monitoring multiple harmonics can provide a more comprehensive view of dynamic processes occurring at the crystal surface (22).

This is particularly useful in studying time-dependent events, such as dynamic adsorption/desorption processes, phase transitions, and the evolution of surface properties over time.

### 2.2.1 Properties of QCM

#### 2.2.1.1 Piezoelectric effect

When pressure is applied to the surface of some crystals, the crystals produce energy in proportion to the applied pressure. Conversely, if energy is applied to the same crystals, dimensional changes occur on the surface of the crystals. When the energy is removed, the crystals return to their original size. This phenomenon is called the piezoelectric effect (4). This property, is also related to the crystallographic properties of substances, was first reported in the literature in 1880 by Pierre and Jacques Curie (23). Quartz crystals display piezoelectric characteristics, enabling them to produce an electrical charge when exposed to mechanical stress or mechanical deformation. Conversely, they also undergo mechanical deformation in response to an electric field. These unique properties are attributed to the crystal's asymmetric molecular structure. When a mechanical force is applied on a quartz crystal, it displaces the crystal lattice, resulting in the production of electric charges on the crystal's surface (23). The magnitude of the electric charge generated is directly proportional to the applied force, allowing quartz crystals to convert mechanical energy into electrical signals. Conversely, when a quartz crystal is subjected to an electric field, it undergoes a mechanical deformation due to the reorientation of the asymmetric crystal lattice (4). This is termed the converse piezoelectric effect and enables quartz crystals to drive mechanical components in various devices (4). Piezoelectric materials are characterized by their ability to exhibit the piezoelectric effect. The fundamental operating principle of a QCM revolves around the piezoelectric properties of quartz crystals.

#### 2.2.1.2 Sauerbrey equation and mass sensitivity of QCM

The Sauerbrey equation is essential for QCM measurements to estimate mass changes resulting from processes such as adsorption, desorption, and thin film deposition. It serves as the basis for quantifying these mass changes and provides an

understanding of the relationship between frequency shifts and surface interactions (24).

The Sauerbrey equation establishes a linear relationship between the frequency change and the mass change on the crystal's surface. It assumes that the deposited mass layer is rigid and homogeneous, and the relationship is valid within the linear range of the crystal's response. The Sauerbrey equation also assumes that the deposited mass layer is thin, rigid, and uniformly covers the entire surface of the crystal. This assumption is essential for the validity of the Sauerbrey equation (7). The Sauerbrey equation provides a means of estimating the mass sensitivity of the QCM system. By knowing the fundamental resonant frequency of the crystal and its physical properties (density and shear modulus), the mass sensitivity of the crystal can be calculated and enables the quantification of mass changes induced by various interactions (17).

$$\Delta f = -\frac{2f_0^2}{S_A\sqrt{\rho_q \mu_q}}\Delta m$$

The core resonant frequency of the QCM is represented by $f_0$, with the crystal's density indicated by ρq, which is 2.648 g/cm$^3$. The shear modulus, a defining characteristic of AT-cut quartz, is denoted by μq and has a value of 2.947 × 10$^{11}$ g/cm·s$^2$. The active area of oscillation is symbolized by A, while $C_f$ stands for the Sauerbrey constant relating to mass sensitivity. Variations in mass on the QCM's surface are expressed as Δm, causing a consequential alteration in the frequency, quantified as Δf (7). The mass sensitivity of a QCM refers to its ability to detect minute mass changes on its surface, and it is determined solely by the core resonant frequency of the QCM crystal, which is a critical aspect of its operation principle. According to the Sauerbrey equation, QCM mass sensitivity is directly related to the fundamental resonant frequency of the quartz crystal used in the device (25). In general, the higher the fundamental frequency of the crystal, the more sensitive it is to mass changes. A 5 MHz crystal, for example, will exhibit a mass sensitivity of 17.7 ng/(cm$^2$•Hz), while a 10 MHz crystal will display a mass sensitivity of 4.4 ng/(cm$^2$•Hz). The mass sensitivity

of QCM plays a crucial role in various applications where precise detection of mass is needed even in nanogram level (20,26,27).

The study suggests that the multiplication of the minimum detectable mass and the acceleration on it remains constant in QCM and beam balances (25). The mass sensitivity coefficient of QCM sensors increases quadratically with frequency, leading to higher sensor sensitivity at higher frequencies. As a result, there is a notable rise in sensitivity or frequency shift per unit of surface mass density acquired.

#### 2.2.1.3 Kanazawa equation

The Kanazawa equation is a pivotal formula used in the operation of QCM devices when they are utilized within liquid environments (17). This equation forms the theoretical basis for understanding how changes in frequency of the quartz crystal are related to changes in the properties of the contacting liquid, particularly its density and viscosity. The Kanazawa equation is derived from an extension of the Sauerbrey equation (28). The Kanazawa equation adapts the relationship between mass and frequency shift for operating with liquids by incorporating liquid density (ρL) and viscosity (ηL) into the calculation. Kanazawa's equation for a liquid medium can be written as:

$$\Delta f = f_0^{3/2} \left( \frac{\rho_L \eta_L}{\pi \rho_q \mu_q} \right)^{1/2}$$

where Δf represents the frequency change of the quartz crystal, $f_0$ is the fundamental resonance frequency of the crystal in the absence of the liquid, Zq is the acoustic impedance of quartz, and ρLηL represents the product of the density and viscosity of the liquid, implying a property known as the "acoustic load" when a QCM is immersed in a liquid.

The product of the square root of liquid density and viscosity is significant because it describes the acoustic load presented by the liquid, which affects the propagation of

the acoustic wave generated by the QCM. A higher acoustic load from the liquid results in a larger decrease in resonant frequency, providing a direct measure of the combined density and viscosity effects (28,29).

This equation allows to calculate viscoelastic properties of the liquid and analyze these properties in real-time, also providing insights into biochemical and material interactions at the sensor-liquid interface, making the QCM a powerful tool for studying the dynamics of liquid-based systems (29).

#### 2.2.1.4 Density and shear modulus

In QCM, density refers to the mass per unit volume of the quartz crystal. The density of the quartz crystal is a crucial parameter in the Sauerbrey equation. The density of quartz is approximately 2.65 g/cm³, and this value is utilized in the Sauerbrey equation to calculate the mass sensitivity of the crystal and to estimate mass changes based on frequency shifts (27).

The shear modulus represents the material's resistance to shear deformation and is a measure of the stiffness of the quartz crystal. In the Sauerbrey equation, the shear modulus is included in the denominator under the square root term, influencing the relationship between frequency change and mass change. For quartz, the shear modulus typically ranges from $2.947 \times 10^{11}$ Pa to $3.106 \times 10^{11}$ Pa, and this parameter is essential in the calculation of mass sensitivity and the interpretation of frequency shifts in QCM measurements (30).

#### 2.2.1.5 Impedance conductance and phase angle

Piezoelectric sensor research is divided into two main categories: active researc and passive research. The active approach involves connecting the sensor to an oscillator amplifier circuit, while the passive method is linking the piezoelectric crystal to an impedance or spectrum analyzer. An impedance analyzer is a specialized electronic instrument which is used for measurement of the electrical impedance of

electronic components, circuits, or materials (31). It is designed to analyze the complex impedance of a device under test over a range of frequencies. The impedance analyzer typically provides information on resistance (R), reactance (X), and phase angle, allowing for a comprehensive understanding of the electrical behavior of the component or material being tested (32). In the passive method, sine waves of varying frequencies are applied to the crystal, and its output signals are recorded to acquire impedance, admittance, and phase angle. Impedance refers to the resistance that a circuit or device offers to the passage of an alternating current. It is represented as Z = R + Xi, comprising both resistance and reactance. The real component signifies dissipated energy, while the imaginary component denotes stored energy (33). The mechanical representation in piezoelectric sensor applications can be described using the Worth–Van Dyke (BVD) equivalent circuit, where resonance occurs when the imaginary part of the impedance equals zero. Conductance, on the other hand, is the reciprocal of resistance. It measures how well a substance can conduct electricity. In contrast to impedance, which is applicable to alternative current (AC) circuits, conductance is often used in the context of direct current (DC) circuits. Conductance (G) can be calculated from impedance (Z) (34).

The phase angle refers to the phase relationship between the excitation voltage and the mechanical response of the quartz crystal. It can be described as a measure of the time delay between the excitation signal and the response signal. It indicates the relative timing of the oscillations between the input and output signals when an alternating voltage is applied to the quartz crystal, it causes the crystal to vibrate (31). In QCM applications, the phase angle is an important parameter as it provides information about the viscoelastic properties of the material or substances deposited on the surface of the quartz crystal (30). A change in the phase angle can signify alterations in the viscoelastic characteristics usually a higher phase angle suggests a more significant viscoelastic or damping effect of the deposited film or substance on the crystal. Therefore, studying the changes in phase angles allows for an understanding of a material's resistance or fluidity. A higher viscoelastic response suggests lower rigidity and increased dissipation, whereas a smaller shift in phase angle indicates more solid-like and less dissipative behavior (15).

In practice, if the phase angle increases, it could be indicative of a softer, more viscoelastic layer, whereas little to no change in the phase angle might suggest a more rigid, mass-dominated interaction. This analytical capability makes the QCM an invaluable tool for the detailed characterization of surface interactions, particularly those involving complex, viscoelastic materials (35). Therefore, in QCM applications, the phase angle serves as a key metric for understanding the dynamic interactions between the quartz crystal and the substances in contact with its surface.

## 2.3 Measurement of Blood Coagulation by QCM

One of the key advantages of using QCM in blood coagulation measurements is its high sensitivity to minute mass variations, which enables the detection of early, tiny clotting events that might remain undetected by conventional methods. By observing frequency changes in the crystal oscillator, QCM characterizes the viscoelastic properties of the clotting blood, delivering comprehensive data, including clot formation kinetics and structure, which are important keywords of hemostatic function (6). Additionally, it offers continuous data monitoring, which is very beneficial because in surgeries, when the patient is given anticoagulants, hemostatic balance is disrupted, and it is important to monitor blood flow and coagulation parameters in short intervals. Furthermore, QCM can measure the effects of different factors, such as temperature and shear stress, on clot formation, providing insights into the underlying mechanisms of coagulation. Another merit of the QCM method is its capacity to simulate various physiological conditions. This is critical for the development of blood-contacting medical devices, as it allows to carefully assess surface-induced coagulation under flow conditions that closely mimic those within the human vessel (5).

In addition to the empirical advantages, QCM can be preferred for its low sample volume requirement, making it an ideal technology for pediatric or neonatal testing, where sample conservation is essential. One of advantages of utilizing QCM in blood coagulation is, it can measure the process independent from optical limitations. In spectrophotometric measurements, it is not possible to monitor coagulation with

whole-blood samples due to optical interference from red blood cells. It offers the prospect of rapid, on-site blood coagulation testing, bridging the gap between benchtop research and bedside patient care. In conclusion, the innovative use of QCM in blood coagulation measurements stands out due to its high sensitivity, capacity to mirror in vivo conditions, economy in sample volume, and the comprehensive data it provides. Therefore, it has surfaced as a promising tool for the advanced hemostatic assessments, facilitating a deeper understanding and potentially revolutionizing the management of coagulopathies in the clinical setting.

There are several researches regarding to coagulation in the literature, beginning with research focused on frequency shifts associated with mass changes during clot formation. Muramatsu et al. (1991) was among the first to demonstrate QCM's utility in detecting coagulation, monitoring mass accumulation on the sensor through frequency (36). Building on this work, Cheng et al. (1998) refined QCM's sensitivity, capturing more subtle mass changes during plasma coagulation (37). Although this advancement expanded QCM's applicability, it remained as only fundamental frequency measurements, restricting insights into mechanical characteristics of clots.

In 2000, Vikinge et al. introduced dissipation (D) measurements alongside frequency shifts on QCM, enabling a dual-parameter approach that captured both mass accumulation and viscoelastic properties, offering a clearer understanding of clot formation (38). This work, however, continued to rely on single-frequency analysis, limiting the complexity of insights obtainable from the data.

Surface coatings on the QCM sensor have played a significant role in enhancing sensitivity and specificity for coagulation studies. Andersson et al. (2005) explored various coatings, including polymethyl methacrylate (PMMA), polyethylene terephthalate (PET), and polydimethylsiloxane (PDMS), demonstrating that these materials could stabilize the QCM signal and reduce interference (39). PMMA and PET offered rigid surfaces, while PDMS's elasticity allowed for sensitive detection of clot structure changes during coagulation. Although these materials improved sensor

interaction with blood samples, this study remained limited to single-frequency measurements, leaving multi-frequency approaches unexplored.

A significant development in QCM-based coagulation research field came with Munawwar Hussain's body of work, which introduced QCM-D in hemostasis studies using various coating materials for improved performance. In 2013, Hussain investigated QCM's potential for measuring prothrombin time (PT) by using polyethylene nanoparticle coatings on a 5 MHz QCM sensor (40). This approach provided real-time PT measurements with accuracy comparable to standard clinical methods, highlighting the potential for QCM-D in clinical settings. Following this, Hussain's 2015 study extended QCM-D applications to activated partial thromboplastin time (aPTT) and Prothrombin Time (PT) assays on human whole blood, using a 10 MHz transducer with a polyvinylpyrrolidone-divinylbenzene (PVP-DVB) coating to improve biocompatibility and sensor stability (41,42). This work established QCM-D as a promising alternative to standard coagulometers for monitoring coagulation in real-time.

Hussain continued to innovate with QCM-D in 2015 by developing a method for thrombin time (TT) measurements in human plasma (43). Using the same 10 MHz transducer and PVP-DVB coating, he demonstrated that QCM-D could yield reliable TT measurements, supporting its clinical relevance. Additionally, in 2014, he showed that QCM-D could achieve heightened sensitivity compared to standard coagulometers in plasma hemostasis assays, particularly at higher coagulation sensitivity thresholds (44). His 2016 review consolidated these findings, emphasizing the importance of coating materials, particularly PVP-DVB, in achieving stable and reproducible coagulation measurements (45).

In parallel, studies continued exploring other coatings. Müller et al. (2010) focused on polyethylene (PE) for its anti-fouling properties, which minimized non-specific protein adsorption and improved QCM signal clarity, essential for accurate coagulation measurement (46). Lakshmanan et al. (2013) examined polystyrene

coatings, which provided a hydrophobic surface that enhanced signal stability by reducing unintended protein interactions (47).

Although significant progress has been made, most QCM studies in coagulation research remains limited to single-frequency analysis, constraining the ability to capture complex dynamics in clot formation. Multi-frequency QCM approach gives the opportunity to analyze multiple harmonics, offers an enhanced methodology that can reveal a more detailed view of clot viscoelastic properties over time. Several studies have investigated blood coagulation using quartz crystal microbalance (QCM); however, none have employed a multi-frequency approach, with analyses conducted exclusively at the fundamental frequency.

In this study, QCM sensors were coated with Low-Density Polyethylene (LDPE) and PMMA. These coatings are crucial for enhancing the sensitivity and specificity of the sensor to biological materials. LDPE is known for its flexibility, while PMMA provides a more stable and rigid coating. However, both materials have distinct mechanical properties that influence the sensor's performance, making it important to assess their efficacy in blood coagulation studies. By comparing the effectiveness of these polymer coatings, this study aims to optimize the QCM sensor’s functionality for monitoring the viscoelastic properties of blood clots.

# 3 MATERIALS AND METHODS

## 3.1 Materials

### 3.1.1 Chemicals

Low Density Polyethylene (LDPE; LyondellBasell Cat no: Alathon l5645) was gifted from Hayim Pinhas Company, Istanbul Türkiye. Xylene Acetone (Galenik, #67-64-1), Polymethyl methacrylate (SIGMA-ALDRICH 200336-50G #MKCF0391), Hydrogen peroxide (SIGMA-ALDRICH, #STBG1775V), Sulfuric acid (SIGMA 1.00713.2500), 18 mm and 15 mm cover slides (ISOLAB) were obtained from Acıbadem Mehmet Ali Aydinlar University research laboratory stock. Platelet Poor Plasma (PPP) (DIAGON cat no: 91010), aPTT test reagents (DIAGON, 72012) and 0.025 M $CaCl_2$ solution (DIAGON, 41048) were gifted from Farmasina Company.

### 3.1.2 QCM

Ti/Au AT-cut QCMs with 10 MHz resonance frequency (Novatech Srl.) with 14 mm diameters were used. These AT-cut 35° 15'± 3' piezoelectric quartz crystals, resonating at a frequency of 10 MHz, are optimally crafted for biosensing applications in liquid environments.

## 3.2 Methods

### 3.2.1 Preparation of QCM for aPTT measurements

QCM should be totally cleaned after every use with sample to eliminate any biological material on the surface as well as it should be clean before operating with. To wash QCM, standard piranha solution was used (47). It was prepared as, mixing concentrated Sulfuric acid and %3 Hydrogen peroxide at 3:1(3mL to 1mL) ratio. Piranha solution was diluted to %10 by adding 4 mL of piranha solution into 36 mL

of deionized water. QCM crystal was cleaned with piranha solution before and after the experiments. After pouring piranha solution on QCM, waited for 30 minutes to operate. After, QCM crystal was rinsed with deionized water several times to remove remaining traces of the cleaning solution. Last, QCM was air dried with nitrogen gas. After cleaning, QCM was coated with LDPE-Xylene and %4 PMMA-Acetone solutions. LDPE-xylene solutions were prepared as 0.1gram of LDPE were weighed and mixed with 10 mL of xylene in beaker. Beaker was put on magnetic stirrer with stirring rod in, heat was adjusted to 150 °C. Beaker was sealed with aluminum foil and solution was stirred overnight for LDPE to completely dissolve.

For coating, 50μL %1 LDPE- xylene solutions were dropped on cover slides and coating process was operated with spin coater (SCS 6800 Spin Coater Series) in 3000rpm for 120 seconds. Cover slides were cut, and samples were examined under Scanning Electron Microscope (SEM) (Thermo scientific Quattro S) for thickness measurement. %4 PMMA-Acetone solution was prepared as; 0.16 gram of PMMA was weighed and mixed with 4 mL of acetone in a bottle. A stirring rod was placed inside the bottle and the bottle lid was closed. The mixture was placed on magnetic stirrer and PMMA was dissolved in acetone for 2 hours. %4 PMMA-acetone solution was dropped on cover slides as 70 μL, and coating process was operated with spin coater (SCS 6800 Spin Coater Series). Cover slides were coated at 3000 rpm for 120 seconds. Cover slides were cut, and samples were examined under Scanning Electron Microscope for thickness measurement. QCMs were coated with LDPE-Xylene and %4PMMA-Acetone solutions same as the cover slides.

### 3.2.2 Preparation of samples

Two sets of samples were used in this study. The first set consisted of PPP samples treated with undiluted aPTT test reagent and $CaCl_2$ (N). The second set used the same plasma samples, but the aPTT reagent was diluted to 50% with injection-grade water and then combined with undiluted plasma and $CaCl_2$ for measurement (D).

### 3.2.3 Experimental setup of aPTT test on QCM

QCM was placed on flow cell and connected to impedance analyzer (KEYSIGHT 4990). A custom MATLAB code was utilized for data acquisition and analysis; however, detailed specifications of the code are not provided in this thesis. Before coating, fundamental resonance frequency (10MHz) was measured regarding the MATLAB code. Due to inconsistencies and challenges in achieving a uniform LDPE coating, as observed in SEM images, aPTT measurements were instead conducted using a PMMA-coated QCM surface. After it checks out, QCM was coated with 4% PMMA acetone solution and fundamental resonance frequency was measured again. After measurement, 80 µL of PPP was dropped on top of QCM at room temperature. Fundamental resonance frequency and different harmonics on Table 1. were scanned for phase angle and peak points of each frequency with related MATLAB code. Peak points were noted for continuous reading. Window sizes for continuous reading were determined as 2000,6000,10.000,14.000,18.000 and 22.000 Hz. With the same code, conductance of PPP on coated QCM was measured as scanning Fundamental resonance frequency and different harmonics with window sizes from Table 1. Start and end frequency of each graph was noted, and peak points were calculated as $(F_{Start}+F_{End})/2$. Window sizes for continuous reading were calculated as $F_{End}-F_{Start}$. Each data was noted and put into another MATLAB code, for scanning different harmonics. Odd numbers have peak data input and even numbers have conductance data. All data was interpreted.

Table 1. Frequency and window size for Impedance and Conductance Measurement

| Frequency (HZ) | Window Size |
|---|---|
| 10.000.000 | 100.000 |
| 30.000.000 | 300.000 |
| 50.000.000 | 500.000 |
| 70.000.000 | 700.000 |
| 90.000.000 | 900.000 |
| 110.000.000 | 1.100.000 |

After frequency and window size determination, continuous reading from impedance analyzer was initiated with MATLAB. After reading starts, 80 μL of aPTT reagent (undiluted or %50 diluted) was added to PPP on QCM and incubated for 3 minutes while reading continues. After incubation, 80 μL of 0.025 M $CaCl_2$ (same in all experiments) was added on QCM, and process was traced for 1 hour.

### 3.3 Curve Generation For Analysis With PYTHON

The frequency and time data obtained from impedance analyzer were transformed into a standard curve (Figure 1) using a PYTHON script, allowing for detailed analysis and calculation of key clotting parameters. This curve visualizes the clotting process by plotting frequency changes over time, providing insights into clotting dynamics with high temporal resolution.

The Python code calculates several essential parameters:

- Clotting Time – This is the time elapsed from calcium addition (marked by the second peak) until the frequency crosses the baseline level, indicating the start of clotting.
- Maximum Clot Firmness (MCF) – MCF is determined as the difference between the highest and lowest frequency values during the clotting process, representing the stability and firmness of the clot.
- Area Under the Curve (AUC) – AUC is calculated as the area between the clotting curve and a reference tangent line drawn from the baseline frequency. This area represents the cumulative effect of clot formation over time and provides additional insights into the clotting dynamics.

The script employs peak detection, baseline adjustments, and spline interpolation techniques to accurately identify these parameters, allowing precise analysis of the clotting process. This approach enables continuous tracking of clot formation and progression, as shown in Figure 1, where calcium addition, baseline crossing, and AUC are clearly marked for visualization and interpretation of clotting behavior.

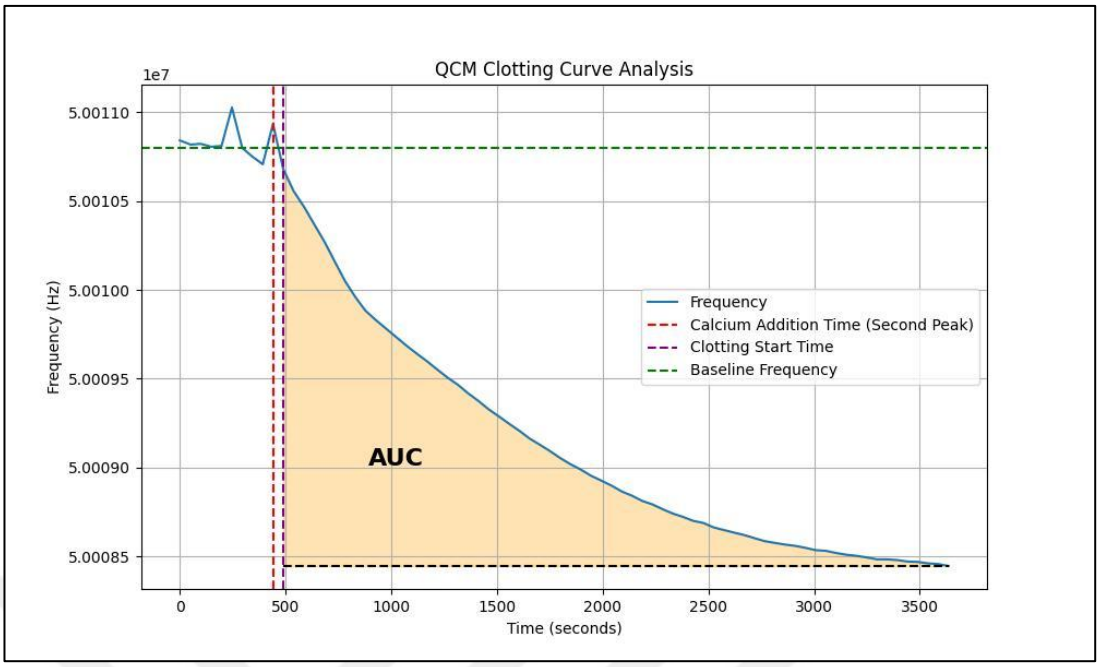


Figure 1. Demonstration of Sample Curve Analysis with PYTHON Script.

Result of the script showing Time (seconds) and Frequency (Hz) on a graph and determines baseline Frequency (green line), Calcium addition time (orange line), clot starting time (purple line) and calculates AUC.

### 3.4 Investigation of Viscoelastic Properties

The modified 3-Layer Kelvin-Voigt Model, fitted using a modified version of the Nelder-Mead simplex algorithm was employed to analyze the shear modulus (μ) and shear viscosity (η) of blood PPP clots in both Normal and Diluted samples (50). This model incorporates a three-layer system to account for the mechanical properties of the clot, considering both elasticity and viscosity contributions at different layers (50). The data fitting was performed using MATLAB routines, incorporating boundaries to ensure that the parameter space was appropriately constrained, enhancing the model's reliability and robustness.

The 3-Layer Kelvin-Voigt Model is a mechanical model used to describe the viscoelastic behavior of complex materials, such as biological tissues or clots, under stress (50). This model is particularly useful in applications involving QCM measurements, where understanding the viscoelastic properties of thin films, such as fibrin clots. The Kelvin-Voigt model is a standard viscoelastic model that consists of

a purely elastic spring and a purely viscous dashpot arranged in parallel . The 3-Layer Kelvin-Voigt Model extends this concept by considering three distinct layers, each represented by a Kelvin-Voigt element, to capture the complex, layered structure of biological samples (51). Layer1 (Surface Layer) represents the sensor surface. This layer is typically sensitive to surface properties and adsorbed molecules. Layer 2 (Intermediate Layer) captures the properties of the bulk of the clot. This layer is primarily responsible for the mechanical stability and viscoelastic behavior of the clot. Layer 3 (Substrate Layer) represents the outermost layer, where the interactions between the clot and the surrounding environment occur. This layer is crucial for understanding how the environmental changes as the clot is formed. Each layer in the model is characterized by its own elastic modulus and viscosity. The combination of these three layers allows the model to capture both the elastic and viscous properties of the material, providing a comprehensive description of its viscoelastic behavior under different conditions (51).

The Nelder-Mead algorithm, also known as the Nelder-Mead simplex method, is a popular optimization technique used for finding the minimum of a function in a multidimensional space (52). This method is particularly well-suited for optimization problems where the function is not differentiable or has discontinuities, which makes traditional gradient-based optimization techniques less effective. The Nelder-Mead algorithm is a heuristic search method that uses a simplex, which is a geometric figure. The algorithm iteratively modifies the simplex to explore the search space and converge to a local minimum of the function.

# 4 RESULTS

## 4.1 SEM Results of LDPE Coating

Penetration depth is a parameter that needs to be considered when operating with QCM in liquids. Penetration depth refers to the distance into a medium (such as a liquid or a thin film) at which the acoustic shear wave generated by the oscillating quartz crystal decays to 1/ $e$ (approximately 37%) of its initial amplitude and it is inversely proportional to square root of resonance frequency (49). Higher frequency results in a shorter penetration depth because the wave decays faster.

$$\delta \propto \frac{1}{\sqrt[2]{f_0}}$$

For instance, at room temperature, the penetration depth of a shear wave in water for a 10 MHz crystal is approximately 180 nanometers.

In SEM images for LDPE coating, it was observed that thickness of coated film is not in the range of penetration depth, and not stable within and between samples. It was seen that thickness was around 200+ nanometers for one sample (Figure 2. A) and there was thickness film variety for another sample, being 225, 165, 198 nms (Figure 2. B). On the other hand, when operating with LDPE solution, it was hard to make observations under SEM because of the nature of LDPE. Not all samples were not representing a uniform layer on the surface, material was stretched and prolonged towards the surface (Figure 2. C).

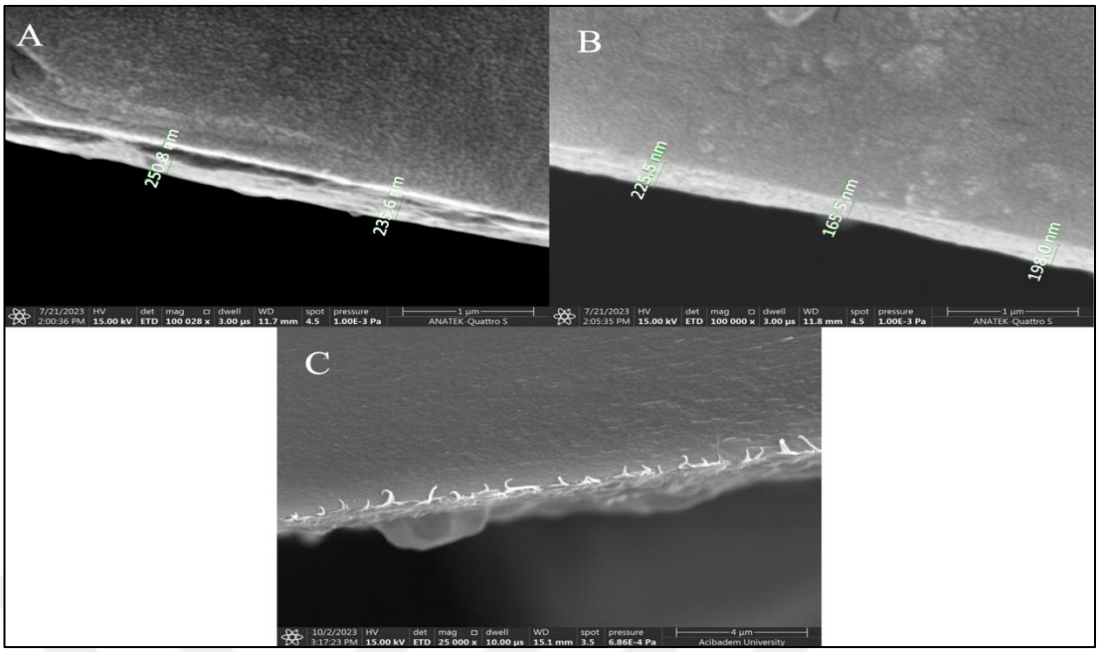


Figure 2. SEM result images of LDPE-xylene coating.

A) LDPE film thickness on cover glass sample 1. B) LDPE film thickness on cover glass sample 2. C) LDPE film thickness on cover glass sample 3

## 4.2 SEM Results of PMMA Coating

Samples coated with PMMA thickness was recorded in the range of penetration depth of QCM. Results were 154.9, 152.3 nms (Figure 3. A) for one sample and 162.7, 161.4, 162.5 nms (Figure 3. B) for another sample. To be sure, imaging was done for 4 different samples, resulted in similar numbers as in the range of 145-165 nms. On the other hand, PMMA samples represented more stable and consistent results compared to LDPE samples, did not stretch or broke on the surface.

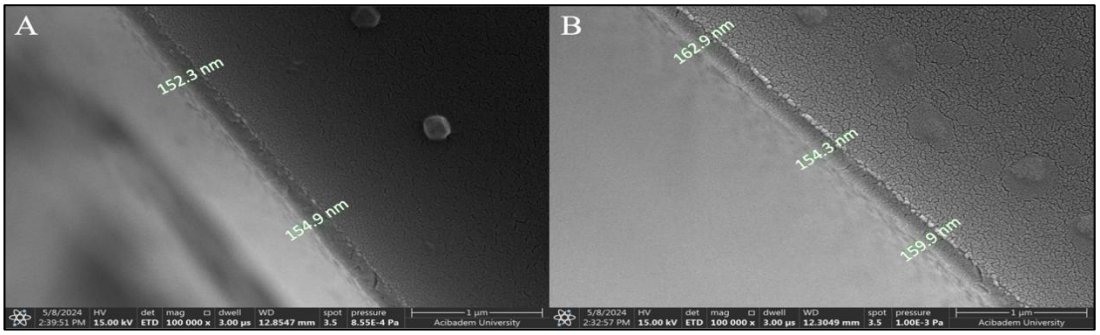


Figure 3. SEM result images of PMMA- Acetone coating.

A) PMMA film thickness on cover glass sample 1. B) PMMA film thickness on cover glass sample 2.

### 4.3 Curve Analysis

An unpaired t-test was used to compare clotting time, maximum clot firmness, area under the curve (AUC), thickness, shear viscosity, and shear modulus parameters between the normal (N) and diluted (D) aPTT reagent groups. Results are presented as mean ± SD, along with the t-statistic, degrees of freedom and p values. This reporting format provides a comprehensive understanding of the data by indicating both central tendency and variability (mean ± SD) and the statistical significance of the comparisons (t, df, p). Statistical analyses and graph preparations were conducted using GraphPad Prism version 5.0.0 for Windows (GraphPad Software, Boston, Massachusetts, USA, 2007) (58).

#### 4.3.1 Clotting time

The results of the clotting time analysis demonstrated statistically significant differences between the N and D sample groups at certain harmonic frequencies. For the measurement at 10 MHz frequency, the mean clotting time for N samples was 51.58 ± 3.4 seconds, while for D samples it was 145.7 ± 1.12 seconds ($t = 47.30$, $df = 3$, $p < 0.0001$). Similarly, for the 30 MHz frequency, the mean clotting time for N samples was 50.31 ± 0.63 seconds, compared to 145.8 ± 1.27 seconds for D samples ($t = 116.2$, $df = 4$, $p < 0.0001$). At 50 MHz, N samples had a mean clotting time of 48.02 ± 0.82 seconds, while D samples showed the value of 146.7 ± 2.06 seconds ($t = 78.92$, $df = 3$, $p < 0.0001$).

These findings highlight the significant impact of diluted aPTT reagent on clotting time across these frequencies (Figure 4). Diluting the aPTT reagent generally slows down the clotting process, leading to a longer clotting time. This is because a lower concentration of clotting activators (such as phospholipids and other cofactors in the reagent) results in a weaker or delayed activation of the intrinsic clotting pathway, extending the time it takes for clot formation to initiate and reach completion.

Based on the data, clotting time calculations for 70 MHz, 90 MHz, and 110 MHz frequencies could not be performed for all measurements due to the curve characteristics not aligning with the specific standards set in the Python code for reliable analysis. Although curves are visible for these frequencies, they do not meet the defined criteria for peak detection and baseline crossing necessary to calculate clotting time accurately. All measurements were performed in triplicate (n = 3).

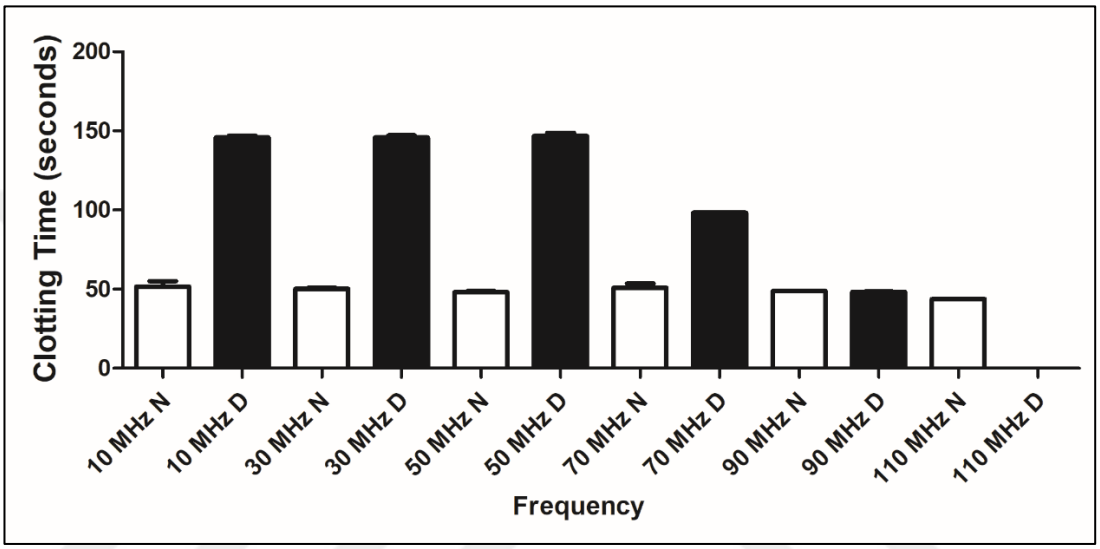


Figure 4. Clotting Time (seconds) for Different Harmonic Frequencies Between N and D Group of Samples.

Significant differences were observed between N and D groups at 10 MHz, 30 MHz, and 50 MHz harmonic frequencies.

### 4.3.2 Maximum clot firmness (MCF)

The analysis of maximum clot firmness (MCF) revealed significant differences between the N and D sample groups specifically at 30 MHz and 50 MHz but not at 10 MHz unlike the clotting time.

For the 30 MHz frequency, N samples had a mean MCF of 1972 ± 119.3 Hz, while D samples showed a lower mean MCF of 1395 ± 237.3 Hz ($t = 3.760$, $df = 4$, $p = 0.0198$). Similarly, at 50 MHz, N samples displayed a higher mean MCF of 2367 ± 246.7 Hz compared to 1529 ± 306.7 Hz for D samples ($t = 3.687$, $df = 4$, $p = 0.0211$), highlighting a clear difference in clot firmness between the two groups at these

frequencies and shows the dilution effect of aPTT reagent. Dilution may reduce MCF, indicating a less stable or weaker clot. This reduction occurs as the clotting cascade is less robust with diluted reagents, which can result in fewer fibrin cross-links and a weaker fibrin network. As a result, the final clot is softer, with lower firmness, making it less resilient under mechanical forces.

In contrast, no statistically significant difference was observed at the 10 MHz frequency, where the mean MCF for Normal samples was 1464 ± 63.92 Hz, compared to 924.7 ± 256.1 Hz for Diluted samples ($t = 2.888$, $df = 2$, $p = 0.1019$). Although there is a visible difference in MCF, with N samples having a higher mean value than D samples, this difference was not statistically significant.

For the 70 MHz, 90MHz and 110MHz frequencies, clotting time calculations could not be performed for all measurements due to curve characteristics not aligning with the specific standards set in the PYTHON code for reliable analysis. Although curves are visible for these frequencies, they do not meet the defined criteria for peak detection and baseline crossing necessary to calculate clotting time accurately (Figure 4). All measurements were performed in triplicate (n=3)

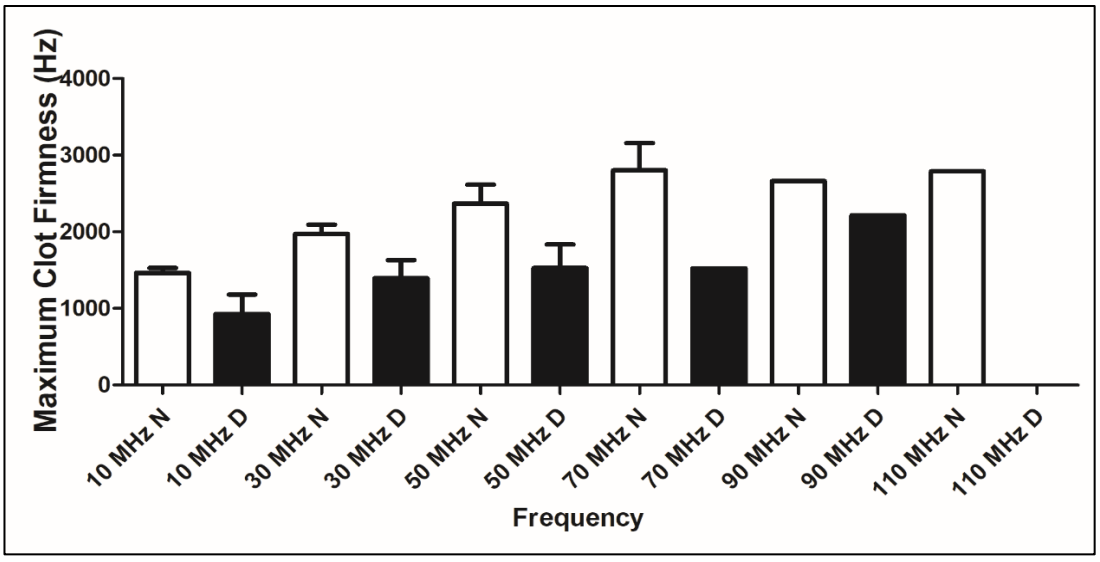


Figure 5. MCF (Hz) for Different Harmonic Frequencies Between N and D Group of Samples.

Significant differences were observed at 30 MHz and 50 MHz. No significant differences were found at other frequencies.

### 4.3.3 Area under the curve (AUC)

The analysis of the area under the curve (AUC) revealed significant differences between the Normal (N) and Diluted (D) sample groups specifically at 30 MHz, but not at 10 MHz or 50 MHz.

For the 30 MHz frequency, N samples had a mean AUC of 1133000 ± 179586 Hz. s, while D samples showed a lower mean AUC of 711009 ± 176384 Hz.s ($t = 2.9$, $df = 4$, $p = 0.0440$), indicating a significant difference between the two groups and suggesting an effect of aPTT reagent dilution.

AUC reflects the overall strength and stability of the clot over time. A diluted reagent may lead to a reduced AUC, as a weaker clot will contribute less to the cumulative clotting response. This effect could be due to both the delayed onset of clotting and the reduced strength of the final clot.

In contrast, at 50 MHz, although N samples displayed a higher mean AUC of 1827000 ± 227042 Hz. s compared to 1389000 ± 197751 Hz.s for D samples, this difference did not reach statistical significance ($t = 2$, $df = 4$, $p = 0.0654$). Similarly, no statistically significant difference was observed at the 10 MHz frequency, where the mean AUC for N samples was 432917 ± 6277 Hz.s, compared to 356193 ± 69791 Hz.s for D samples ($t = 1$, $df = 3$, $p = 0.3015$).

These findings indicate that significant differences in AUC were only observe at 30 MHz, while 10 MHz and 50 MHz did not exhibit statistically significant differences between the N and D samples.

For the 70 MHz, 90 MHz, and 110 MHz frequencies, clotting time calculations could not be performed for all measurements due to the curve characteristics not aligning with the specific standards set in the Python code for reliable analysis.

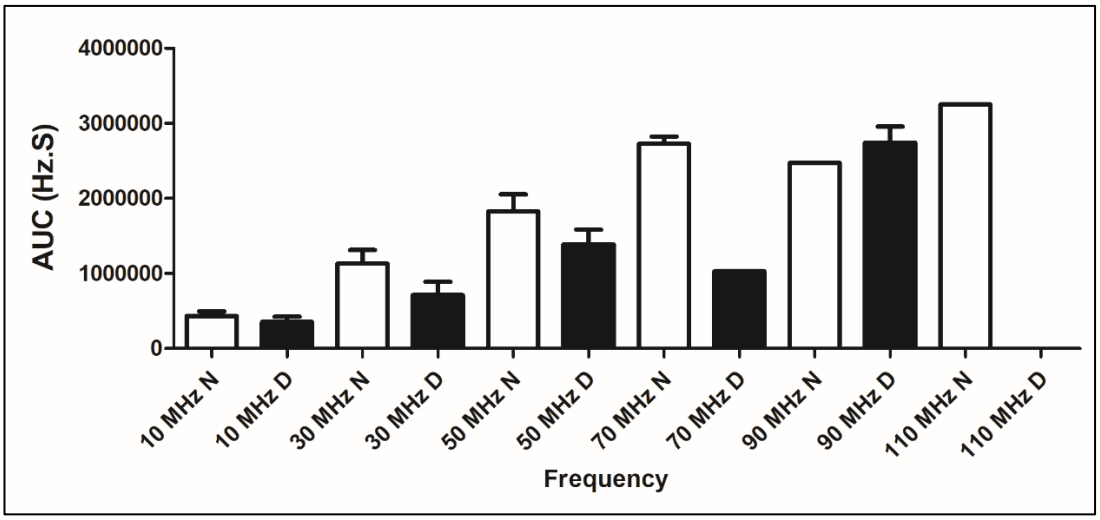


Figure 6. AUC (Hz.s) for different harmonic frequencies between N and D group of samples.

Significant differences were only observed at 30 MHz. No significant differences were found at other frequencies.

### 4.4 Viscoelastic Properties

The dilution of the aPTT reagent has notable effects on the viscoelastic properties of PPP clots, impacting parameters thickness, shear viscosity, and shear modulus which were analyzed using the 3-Layer Kelvin-Voigt Model. For clot thickness, the mean value for the N samples was 14.93 ± 1.02 nm, while for the D samples, it was 15.03 ± 2.04 nm ($t = 0.07583$, $df = 4$, $p = 0.9432$), indicating no significant difference between the two groups.

For viscosity, the N samples had a mean value of 0.001401 ± 0.0003506 Pa·s while the D samples had a mean of 0.001325 ± 0.0002994 Pa·s ($t = 0.2828$, $df = 4$, $p = 0.7914$), illustrating no significant difference between the two conditions. In terms of shear modulus, the Normal samples exhibited a mean of 293901 ± 31296 Pa, contrasting sharply with the Diluted samples, which showed a markedly lower mean of 175170 ± 19026 Pa ($t = 5.615$, $df = 4$, $p < 0.01$), reflecting a significant disparity in clot stiffness between the conditions. The shear modulus (μ1) provides a measure of the clot's elasticity or stiffness, reflecting how well the clot can resist deformation under shear stress. The higher shear modulus values in the N samples indicate that the clots formed under these conditions were more robust and elastic. This suggests that

the clot network was more densely cross-linked, providing greater mechanical strength and resistance to deformation. The lower and more variable shear modulus values in the D samples reflect a reduction in clot stiffness, likely due to the dilution of the aPTT reagent. The diluted reagent may have slowed the coagulation cascade, resulting in clots with weaker fibrin networks or incomplete cross-linking, leading to reduced mechanical strength in clot properties.

Shear viscosity (η1) measures the clot's resistance to flow, reflecting its viscous properties.

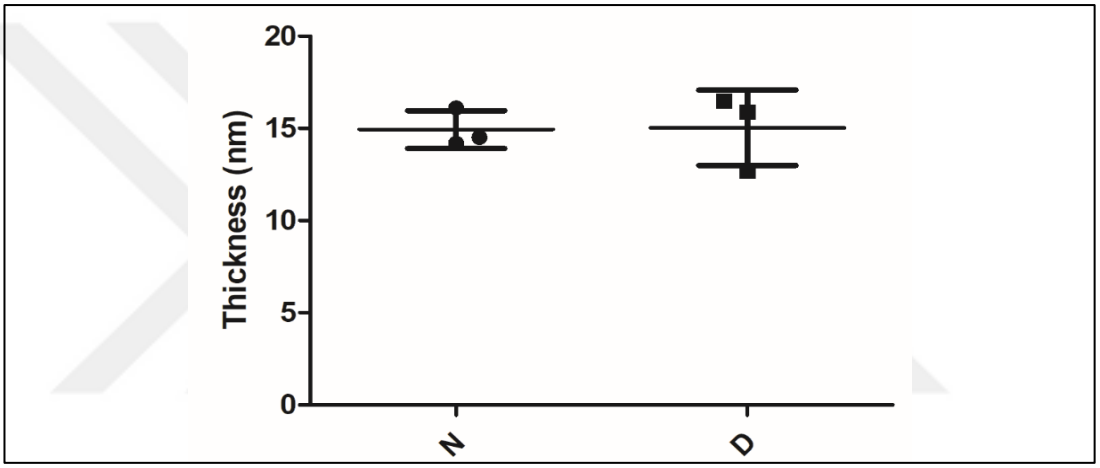


Figure 7. Clot thickness (nm) of N and D group of samples.

No significant difference between the two sample groups were observed.

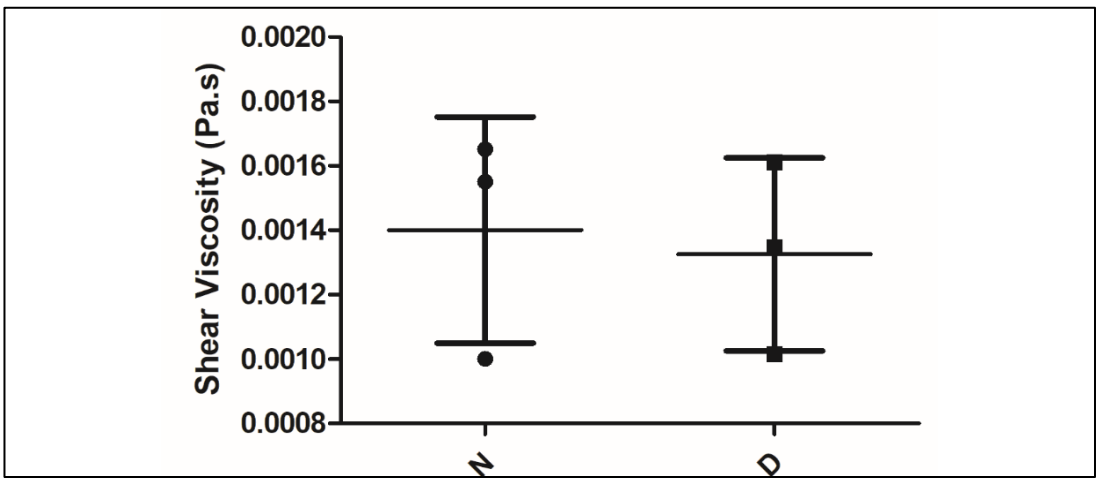


Figure 8. Shear Viscosity (Pa.s) of N and D group of samples.

There was no significant difference between the two sample groups.

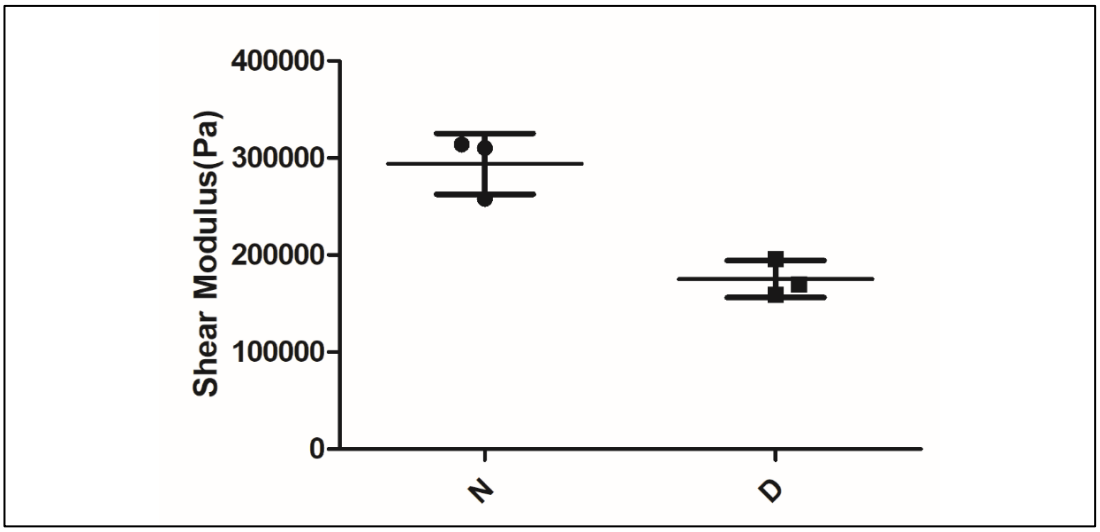


Figure 9. Shear Modulus (Pa) of N and D group of samples.

The mean shear modulus of N samples was significantly higher than the values for D samples.

# 5 DISCUSSION

The findings of this study provide valuable insights into the use of QCM technology for blood coagulation monitoring at different harmonic frequencies. While previous studies on QCM-based coagulation monitoring have focused on fundamental frequencies, this research fills a critical gap by examining the role of higher harmonics, providing more understanding of clot dynamics. Additionally, the comparison of LDPE and PMMA coatings highlights the importance of selecting appropriate materials for sensor performance.

The SEM analysis played a crucial role in evaluating the coating materials used on the QCM sensor. For the LDPE coatings, the results indicated considerable variability in thickness and non-uniform distribution across samples. The thickness of LDPE coatings was often outside the optimal range for QCM applications in liquids, which is determined by the penetration depth of the acoustic wave. This inconsistency likely affected the sensitivity and accuracy of the measurements. The challenges associated with LDPE coatings, such as immediate solidification at room temperature and difficulty in achieving a uniform thin film, suggest that LDPE may not be the most suitable material for our QCM-based coagulation studies.

Conversely, coatings made PMMA dissolved in acetone were found to be more reliable. The SEM images showed that PMMA coatings were more consistent in thickness, falling within the acceptable range for QCM penetration depth. Unlike LDPE, PMMA did not exhibit significant stretching or breaking, providing a more stable surface for QCM measurements. Overall, the results from SEM imaging revealed that PMMA is a more suitable coating material for QCM sensors in coagulation studies due to its uniform thickness and stability within the penetration depth. In contrast, LDPE's inconsistency in thickness and poor film-forming properties limited its utility, promotes the importance of selecting stable and uniform coatings for reliable QCM performance in liquid environments. The findings also suggest that an automated coating process could further improve consistency, providing a more uniform and controlled application of the coating material, which is critical for

achieving reliable and reproducible results in QCM-based coagulation studies (41-43,45,46).

After establishing the limitations of LDPE coatings and the reliability of PMMA, our research turns to the frequency-dependent analysis of clotting dynamics. By employing higher harmonic frequencies, we were able to achieve more sensitive measurements of clot formation and its mechanical properties. The clotting time analysis revealed statistically significant differences between N and D samples across some tested harmonic frequencies (10 MHz, 30 MHz, and 50 MHz). This indicates that clotting time is highly sensitive to both dilution and the used harmonic frequency. The significant differences observed at tested frequencies suggest that QCM can effectively differentiate between normal and altered coagulation states. The use of higher harmonic frequencies (30 MHz and 50 MHz) provided additional sensitivity, capturing subtle differences that might not be apparent at the fundamental frequency. These findings align with previous literature suggesting that higher harmonics provide better resolution of mechanical properties, such as elasticity and viscosity, which are critical for understanding the viscoelastic behavior of blood clots (22,53).

The MCF results also demonstrated the advantage of higher harmonics in QCM measurements. Significant differences in MCF were observed at 30 MHz and 50 MHz between the Nand D samples, while no significant difference was detected at 10 MHz. This suggests that the ability to detect differences in clot firmness improves with higher frequencies, likely due to the reduced penetration depth and increased sensitivity to surface-bound processes. The use of higher harmonics provided critical insights into clot viscoelasticity and mechanical behavior that were otherwise missed at fundamental frequencies. The increased resolution at 30 MHz and 50 MHz allowed for the detection of more subtle variations in clot firmness and viscosity, underscoring the potential of multi-frequency analysis for more comprehensive coagulation studies (53).

The area under the curve (AUC) analysis provided further evidence for the importance of frequency selection in QCM-based coagulation studies. A significant

difference in AUC was observed at 30 MHz, but not at 10 MHz or 50 MHz. This highlights the complexity of the coagulation process and the need to carefully select the appropriate frequency for different types of measurements. While the 10 MHz and 50 MHz frequencies did not show significant differences in AUC, the 30 MHz frequency did, suggesting that certain frequencies may be more sensitive to specific aspects of coagulation. This variability suggests the need for a multi-frequency approach in QCM analysis to capture the full spectrum of clotting dynamics (45,46).

While higher harmonics provided increased sensitivity in QCM measurements, they also introduced challenges in data interpretation. The raw data obtained from the QCM measurements were analyzed without any data smoothing techniques to preserve the integrity of the data and ensure that all observed effects were real and not artifacts of data processing. However, the higher sensitivity at increased harmonics made the data more susceptible to noise, which, in some cases, made it difficult to interpret the results accurately. Specifically, for some frequencies, the noise was significant enough that our curve-fitting algorithms could not effectively model the data, resulting in difficulties in interpreting certain aspects of the coagulation process (50). The results obtained from the Kelvin-Voigt model and Nelder-Mead algorithm provide valuable insights into the differences in clot properties between N and D samples. The data reveal both significant and non-significant findings across the parameters of clot thickness, shear viscosity, and shear modulus, contributing to our understanding of how dilution affects the coagulation process.

The statistics analysis showed no significant difference in clot thickness between the N and D samples. This suggests that, despite the dilution of the aPTT reagent, the overall structure and formation of the clot, in terms of thickness, remain relatively consistent across the two conditions. This is an important observation, as it implies that clot formation can still occur with similar structural integrity, even when the aPTT reagent is diluted. However, thickness alone does not provide a complete picture of clot functionality or strength, as other mechanical properties, such as elasticity and stiffness, play a critical role in clot stability. When evaluating the viscosity of the clots, the results showed no significant difference between the two groups. Viscosity reflects

the clot's resistance to flow and is a key factor in understanding its mechanical behavior. The similarity in viscosity across both N and D samples suggests that the overall fluidity and flow resistance of the clots are maintained, regardless of reagent concentration. This indicates that while the dilution affects certain aspects of clot formation, it does not have a profound impact on the viscous properties of the clots. In contrast, a significant difference was observed in the shear modulus between the N and D samples. Shear modulus is an indicator of a clot's elasticity or stiffness, representing its ability to resist deformation under stress. The data suggest that clots formed from the normal samples were substantially stiffer and more elastic compared to those from the diluted samples. This finding is crucial, as it highlights the impact of reagent dilution on the mechanical integrity of the clot. The lower stiffness in diluted samples likely reflects a weakened fibrin network, potentially due to the slower or incomplete activation of the coagulation cascade. This reduction in mechanical strength could result in clots that are less stable and more prone to deformation or breakage under physiological stress. The difference in shear modulus between the two conditions suggests that while the overall structure and flow resistance of the clot are preserved, its mechanical strength is compromised by the dilution of the aPTT reagent. This could have important implications for clinical settings where clot stability is crucial, such as during surgeries or in patients with clotting disorders. The reduced stiffness in D samples indicates that the clot may be more susceptible to mechanical stress, which could increase the risk of clot lysis or failure.

These findings emphasize the importance of analyzing both elasticity and viscosity to gain a comprehensive understanding of clot mechanics. While thickness and viscosity provide insights into the general structure and flow properties of the clot, the shear modulus offers critical information about its mechanical strength and resilience. The significant reduction in stiffness in diluted samples underscores the need for careful consideration of reagent concentrations in coagulation assays, as even small changes can have a profound effect on clot integrity.

In summary, the use of the Kelvin-Voigt model and the Nelder-Mead algorithm in this study provided a detailed analysis of clot mechanical properties, revealing

important differences between normal and diluted samples. While thickness and viscosity remained largely unaffected by dilution, the significant decrease in shear modulus highlights the vulnerability of the diluted clots to mechanical stress. This underscores the value of multi-faceted analyses in understanding clot dynamics, where multiple parameters must be considered to fully assess clot functionality and stability. Future research could further explore the implications of these findings in clinical applications, particularly in optimizing reagent concentrations for more robust clot formation in therapeutic contexts.

This study demonstrates the value of multi-harmonic analysis in QCM-based coagulation monitoring, providing a more comprehensive understanding of the clotting process than traditional single-frequency approaches. While lower frequencies provide valuable information about overall coagulation status, higher frequencies offer more detailed insights into the specific properties of clots, such as firmness and viscoelasticity. Future research should continue to explore the use of multiple harmonics and develop standardized protocols for sensor coating and measurement procedures to minimize noise and improve the reliability of QCM data (6).

In conclusion, this study provides significant advancements in the use of QCM technology for coagulation monitoring across different harmonic frequencies. It highlights the importance of both coating materials and frequency selection in achieving reliable and sensitive measurements of clot formation. While PMMA proved to be a more suitable coating material than LDPE, the use of higher harmonics enabled a more detailed analysis of clot dynamics, offering critical insights into clot firmness, viscosity, and mechanical behavior. These findings pave the way for further research into optimizing QCM technology for clinical diagnostics and improving our understanding of the coagulation process in real time.

# 6 CONCLUSION

This study highlights the potential of QCM technology for advanced coagulation monitoring by emphasizing the importance of harmonic frequency selection and coating materials in achieving accurate and reliable measurements. The primary objective was to explore the impact of higher harmonic frequencies (30 MHz and 50 MHz) on the detection of clotting parameters such as clotting time, maximum clot firmness, and area under the curve. The results clearly demonstrate that higher harmonics provide greater sensitivity and resolution, allowing for more consistent detection of significant differences between N and D plasma samples, a feature that is not as evident at fundamental frequencies.

However, the study also identified several limitations that need to be addressed in future research. First, the lack of standardized methods for QCM sensor coating and coagulation measurement presents a challenge for reproducibility and comparability across studies. The variability in coating thickness and uniformity, particularly with LDPE, highlights the need for more controlled and automated coating techniques. Implementing standardized protocols for sensor preparation and measurement procedures will be essential for advancing the use of QCM in clinical and research settings. Additionally, all measurements in this study were conducted at room temperature (23-25°C), which is lower than physiological body temperature (37°C). Since coagulation involves a series of temperature-sensitive enzymatic reactions, future studies should incorporate a QCM system with an integrated incubator to maintain physiological temperature conditions. This adjustment could provide more accurate and clinically relevant results, improving the understanding of coagulation dynamics under conditions that closely mimic the human body.

Despite these limitations, this study provides valuable insights into the use of higher harmonic frequencies for QCM-based coagulation monitoring. The results suggest that QCM technology, especially when combined with advanced models like the modified 3-Layer Kelvin-Voigt model, has the potential to offer a more comprehensive analysis of clot formation. By providing detailed measurements of

clot mechanical properties, such as shear modulus and viscosity, the study demonstrates how QCM technology can go beyond traditional and optical methods, which are often affected by sample color and lack real-time viscoelastic monitoring.

The findings from the Kelvin-Voigt model showed that dilution of the aPTT reagent significantly reduces the shear modulus of clots, indicating a weakened fibrin network and reduced mechanical strength. In contrast, the film thickness and viscosity of the clots were not significantly affected by dilution. These results highlight the importance of understanding how reagent concentrations can impact clot formation and structure, offering crucial insights for clinical practice and anticoagulation therapies. The integration of QCM technology with advanced modeling techniques not only provides real-time insights into clot dynamics but also offers a powerful tool for investigating clot properties under different experimental conditions.

This study also aligns with existing literature on plasma viscosity and clot thickness (22, 45, 53, 54), although the higher shear modulus values observed here suggest that the experimental setup captured more detailed mechanical variations (55, 56, 57). The use of higher harmonic frequencies provided increased sensitivity, but also introduced noise, which complicated data interpretation. Future research should explore data smoothing techniques to reduce this noise and improve the accuracy of curve fitting, particularly at higher frequencies.

In conclusion, this study demonstrates the utility of using multiple harmonics in QCM measurements to provide a more detailed analysis of blood coagulation dynamics, while highlighting the critical role of reagent concentration in influencing mechanical properties like shear modulus. By addressing the identified limitations and refining methodology, including temperature control and coating techniques, QCM technology holds the potential to become a powerful tool for both research and clinical coagulation monitoring. The findings further reveal that diluting the aPTT reagent affects the mechanical properties of platelet-poor plasma clots, leading to lowered shear modulus, which suggests that dilution impairs the clotting process by reducing

the availability of key clotting factors, resulting in weaker clots. These results emphasize the importance of reagent concentration in coagulation studies and underscore the value of QCM technology in providing detailed measurements of clot mechanical properties. Future research should explore varying degrees of dilution and other factors influencing clot formation to deepen the understanding of blood coagulation dynamics and their broader implications for clinical practice.

# 7 REFERENCES


1. Palta S, Saroa R, Palta A. Overview of the coagulation system. Indian Journal of Anaesthesia [Internet]. 2014 Jan 1;58(5):515. Available from: https://doi.org/10.4103/0019-5049.144643
2. Papageorghiou AT, Kennedy SH, Salomon LJ, Altman DG, Ohuma EO, Stones W, et al. The INTERGROWTH-21st fetal growth standards: toward the global integration of pregnancy and pediatric care. American Journal of Obstetrics and Gynecology [Internet]. 2018 Feb 1;218(2):S630–40. Available from: https://doi.org/10.1016/j.ajog.2018.01.011
3. Nonoyama A, Garcia-Lopez A, Garcia-Rubio LH, Leparc GF, Potter RL. Hypochromicity in red blood cells: an experimental and theoretical investigation. Biomedical Optics Express [Internet]. 2011 Jul 1;2(8):2126. Available from: https://doi.org/10.1364/boe.2.002126
4. Jandas P, Prabakaran K, Luo J, G DHM. Effective utilization of quartz crystal microbalance as a tool for biosensing applications. Sensors and Actuators a Physical [Internet]. 2021 Aug 4;331:113020. Available from: https://doi.org/10.1016/j.sna.2021.113020
5. Mohammadinejad A, Aleyaghoob G, Nooranian S, Dima L, Moga MA, Badea M. Development of biosensors for detection of fibrinogen: a review. Analytical and Bioanalytical Chemistry [Internet]. 2023 Oct 14;416(1):21–36. Available from: https://doi.org/10.1007/s00216-023-04976-1
6. Efremov V, Lakshmanan RS, O'Donnell J, Killard AJ. Rapid Whole Blood Clot Retraction Assay on Quartz Crystal Microbalance. IEEE Sensors Letters [Internet]. 2021 Jan 1;5(1):1–4. Available from: https://doi.org/10.1109/lsens.2020.3049063
7. Songkhla SN, Nakamoto T. Overview of Quartz Crystal Microbalance Behavior Analysis and Measurement. Chemosensors [Internet]. 2021 Dec 10;9(12):350. Available from: https://doi.org/10.3390/chemosensors9120350
8. Dahlbäck B. Blood coagulation. The Lancet [Internet]. 2000 May 1;355(9215):1627–32. Available from: https://doi.org/10.1016/s0140-6736(00)02225-x
9. Bhattarai A, Shah S, Bagherieh S, Mirmosayyeb O, Thapa S, Paudel S, et al. Endothelium, Platelets, and Coagulation Factors as the Three Vital Components for Diagnosing Bleeding Disorders: A Simplified Perspective with Clinical Relevance. International Journal of Clinical Practice [Internet]. 2022 Aug 27;2022:1–10. Available from: https://doi.org/10.1155/2022/5369001
10. Karki KB, Poudyal A, Shrestha N, Mahato NK, Aryal KK, Sijapati MJ, et al. Factors Associated with Chronic Obstructive Pulmonary Diseases in Nepal: Evidence from a Nationally Representative Population-Based Study. International Journal of COPD [Internet]. 2021 Apr 1;Volume 16:1109–18. Available from: https://doi.org/10.2147/copd.s295321
11. Hadid T, Kafri Z, Al-Katib A. Coagulation and anticoagulation in COVID-19. Blood Reviews [Internet]. 2020 Oct 8;47:100761. Available from: https://doi.org/10.1016/j.blre.2020.100761
12. Raber MN. Coagulation Tests [Internet]. Clinical Methods - NCBI Bookshelf. 1990. Available from: https://www.ncbi.nlm.nih.gov/books/NBK265/

13. Iba T, Levy JH, Warkentin TE, Thachil J, Van Der Poll T, Levi M. Diagnosis and management of sepsis-induced coagulopathy and disseminated intravascular coagulation. Journal of Thrombosis and Haemostasis [Internet]. 2019 Jul 20;17(11):1989–94. Available from: https://doi.org/10.1111/jth.14578
14. Teichman J, Chaudhry HR, Sholzberg M. Novel assays in the coagulation laboratory: a clinical and laboratory perspective. Transfusion and Apheresis Science [Internet]. 2018 Jul 21;57(4):480–4. Available from: https://doi.org/10.1016/j.transci.2018.07.008
15. Efremov V, Killard AJ, Byrne B, Lakshmanan RS. The modelling of blood coagulation using the quartz crystal microbalance. Journal of Biomechanics [Internet]. 2012 Nov 10;46(3):437–42. Available from: https://doi.org/10.1016/j.jbiomech.2012.10.001
16. Alanazi N, Almutairi M, Alodhayb AN. A Review of Quartz Crystal Microbalance for Chemical and Biological Sensing Applications. Sensing and Imaging [Internet]. 2023 Mar 4;24(1). Available from: https://doi.org/10.1007/s11220-023-00413-w
17. Huang, X., Chen, Q., Pan, W., & Yao, Y. (2022, July 7). Advances in the Mass Sensitivity Distribution of Quartz Crystal Microbalances: A Review. https://doi.org/10.3390/s22145112
18. Saad NA, Zaaba SK, Zakaria A, Kamarudin LM, Wan K, Shariman AB. Quartz crystal microbalance for bacteria application review [Internet]. 2014 2nd International Conference on Electronic Design (ICED), Penang, Malaysia. 2014. Available from: https://doi.org/10.1109/iced.2014.7015849
19. Yoshimine H, Sasaki K, Furusawa H. Pocketable Biosensor Based on Quartz-Crystal Microbalance and Its Application to DNA Detection. Sensors [Internet]. 2022 Dec 27;23(1):281. Available from: https://doi.org/10.3390/s23010281
20. Jang IR, Kim HJ. Short Review on Quartz Crystal Microbalance Sensors for Physical, Chemical, and Biological Applications. Journal of Sensor Science and Technology [Internet]. 2022 Nov 30;31(6):389–96. Available from: https://doi.org/10.46670/jsst.2022.31.6.389
21. Kraus PR, Cooper FL, Emmons DH, Ferguson S, McClain RD, Spates JJ. Use of quartz crystal microbalance sensors for monitoring fouling and viscoelastic phenomena in industrial process applications [Internet]. Vol. 175, https://ieeexplore.ieee.org/xpl/conhome/7650/proceeding. 2002. Available from: https://doi.org/10.1109/sficon.2001.968537
22. Speller NC, Siraj N, Regmi BP, Marzoughi H, Neal C, Warner IM. Rational Design of QCM-D Virtual Sensor Arrays Based on Film Thickness, Viscoelasticity, and Harmonics for Vapor Discrimination. Analytical Chemistry [Internet]. 2015 Apr 27;87(10):5156–66. Available from: https://doi.org/10.1021/ac5046824
23. Uchino K. The Development of Piezoelectric Materials and the New Perspective. In: Elsevier eBooks [Internet]. 2017. p. 1–92. Available from: https://doi.org/10.1016/b978-0-08-102135-4.00001-1
24. Pan M, Hong L, Yang J, Xie X, Liu K, Wang S. Fabrication and evaluation of a portable and reproducible quartz crystal microbalance immunochip for label-free detection of β-lactoglobulin

allergen in milk products. Food Science and Human Wellness [Internet]. 2022 Jun 2;11(5):1315–21. Available from: https://doi.org/10.1016/j.fshw.2022.04.015

25. Mecea VM. From Quartz Crystal Microbalance to Fundamental Principles of Mass Measurements. Analytical Letters [Internet]. 2005 Mar 1;38(5):753–67. Available from: https://doi.org/10.1081/al-200056171
26. Vashist SK, Vashist P. Recent Advances in Quartz Crystal Microbalance-Based Sensors. Journal of Sensors [Internet]. 2011 Jan 1;2011:1–13. Available from: https://doi.org/10.1155/2011/571405
27. Lucklum R, Hauptmann P. The quartz crystal microbalance: mass sensitivity, viscoelasticity and acoustic amplification. Sensors and Actuators B Chemical [Internet]. 2000 Nov 1;70(1–3):30–6. Available from: https://doi.org/10.1016/s0925-4005(00)00550-5
28. Horst RJ, Katzourakis A, Mei BT, De Beer S. Design and validation of a low-cost open-source impedance-based quartz crystal microbalance for electrochemical research. HardwareX [Internet]. 2022 Oct 1;12:e00374. Available from: https://doi.org/10.1016/j.ohx.2022.e00374
29. Johannsmann D, Langhoff A, Leppin C. Studying Soft Interfaces with Shear Waves: Principles and Applications of the Quartz Crystal Microbalance (QCM). Sensors [Internet]. 2021 May 17;21(10):3490. Available from: https://doi.org/10.3390/s21103490
30. Naranda J, Bračič M, Vogrin M, Maver U, Trojner T. Practical Use of Quartz Crystal Microbalance Monitoring in Cartilage Tissue Engineering. Journal of Functional Biomaterials [Internet]. 2022 Sep 21;13(4):159. Available from: https://doi.org/10.3390/jfb13040159
31. Pathiraja AA, Weerakkody RA, Von Roon AC, Ziprin P, Bayford R. The clinical application of electrical impedance technology in the detection of malignant neoplasms: a systematic review. Journal of Translational Medicine [Internet]. 2020 Jun 8;18(1). Available from: https://doi.org/10.1186/s12967-020-02395-9
32. Ward LC, Brantlov S. Bioimpedance basics and phase angle fundamentals. Reviews in Endocrine and Metabolic Disorders [Internet]. 2023 Feb 7;24(3):381–91. Available from: https://doi.org/10.1007/s11154-022-09780-3
33. Cseresnyés I, Rajkai K, Vozáry E. Role of phase angle measurement in electrical impedance spectroscopy. International Agrophysics [Internet]. 2013 Oct 21;27(4):377–83. Available from: https://doi.org/10.2478/intag-2013-0007
34. Burda I. Virtual Quartz Crystal Microbalance: Bioinspired Resonant Frequency Tracking. Biomimetics [Internet]. 2022 Oct 8;7(4):156. Available from: https://doi.org/10.3390/biomimetics7040156
35. Qiao X, Zhang X, Tian Y, Meng Y. Progresses on the theory and application of quartz crystal microbalance. Applied Physics Reviews [Internet]. 2016 Sep 1;3(3):031106. Available from: https://doi.org/10.1063/1.4963312
36. Muramatsu H, Kimura K, Ataka T, Homma R, Miura Y, Karube I. A quartz crystal viscosity sensor for monitoring coagulation reaction and its application to a multichannel coagulation detector. Biosensors and Bioelectronics [Internet]. 1991 Jan 1;6(4):353–8. Available from: https://doi.org/10.1016/0956-5663(91)85022-o

37. Cheng NTJ, Chang NHC, Lin NTM. A piezoelectric quartz crystal sensor for the determination of coagulation time in plasma and whole blood. Biosensors and Bioelectronics [Internet]. 1998 Feb 1;13(2):147–56. Available from: https://doi.org/10.1016/s0956-5663(97)00111-5
38. Vikinge TP, Hansson KM, Sandström P, Liedberg B, Lindahl TL, Lundström I, et al. Comparison of surface plasmon resonance and quartz crystal microbalance in the study of whole blood and plasma coagulation. Biosensors and Bioelectronics [Internet]. 2000 Dec 1;15(11–12):605–13. Available from: https://doi.org/10.1016/s0956-5663(00)00125-1
39. Andersson M, Andersson J, Sellborn A, Berglin M, Nilsson B, Elwing H. Quartz crystal microbalance-with dissipation monitoring (QCM-D) for real time measurements of blood coagulation density and immune complement activation on artificial surfaces. Biosensors and Bioelectronics [Internet]. 2004 Nov 12;21(1):79–86. Available from: https://doi.org/10.1016/j.bios.2004.09.026
40. Munawar Hussain, Stefan Sinn1, Martin Zeilinger, Hinnak Northoff, Peter A Lieberzeit, Frank K Gehring. Blood Coagulation Thromboplastine Time Measurements on a Nanoparticle Coated Quartz Crystal Microbalance Biosensor in Excellent Agreement with Standard Clinical Methods. Journal of Biosensors & Bioelectronics [Internet]. 2013 Jan 1;04(04). Available from: https://doi.org/10.4172/2155-6210.1000139
41. Hussain NM. aPTT: 1st Recognition for Human Whole Blood on QCM-D Platform. Pharmaceutical and Biosciences Journal [Internet]. 2015 Sep 29;49–55. Available from: https://doi.org/10.20510/ukjpb/3/i6/87835
42. Hussain M. Prothrombin Time (PT) for Human Plasma on QCM-D Platform: A Better Alternative to "Gold Standard." Pharmaceutical and Biosciences Journal [Internet]. 2015 Sep 8;01–8. Available from: https://doi.org/10.20510/ukjpb/3/i6/87830
43. Hussain NM. Shortened "Thrombin Time" Monitoring on QCM-D: A Better Substitute of "Gold Standard." Pharmaceutical and Biosciences Journal [Internet]. 2015 Oct 30;20–6. Available from: https://doi.org/10.20510/ukjpb/4/i1/87841
44. Hussain M, Northoff H, Gehring FK. QCM-D providing new horizon in the domain of sensitivity range and information for haemostasis of human plasma. Biosensors and Bioelectronics [Internet]. 2014 Dec 3;66:579–84. Available from: https://doi.org/10.1016/j.bios.2014.12.003
45. Hussain NM. QCM-D for Haemostasis Assays: Current Status and Future: A Review. Pharmaceutical and Biosciences Journal [Internet]. 2016 Jan 22;121–32. Available from: https://doi.org/10.20510/ukjpb/4/i1/90386
46. Müller L, Sinn S, Drechsel H, Ziegler C, Wendel HP, Northoff H, et al. Investigation of Prothrombin Time in Human Whole-Blood Samples with a Quartz Crystal Biosensor. Analytical Chemistry [Internet]. 2010 Jan 29;82(5):2164. Available from: https://doi.org/10.1021/ac100170q
47. Lakshmanan RS, Efremov V, Cullen SM, Killard AJ. Measurement of the evolution of rigid and viscoelastic mass contributions from fibrin network formation during plasma coagulation using quartz crystal microbalance. Sensors and Actuators B Chemical [Internet]. 2013 Oct 28;192:23–8. Available from: https://doi.org/10.1016/j.snb.2013.10.081

48. Wasilewski T, Szulczyński B, Dobrzyniewski D, Jakubaszek W, Gębicki J, Kamysz W. Development and Assessment of Regeneration Methods for Peptide-Based QCM Biosensors in VOCs Analysis Applications. Biosensors [Internet]. 2022 May 7;12(5):309. Available from: https://doi.org/10.3390/bios12050309
49. Mukhin N, Lucklum R. QCM based sensor for detecting volumetric properties of liquids. Current Applied Physics [Internet]. 2019 Mar 23;19(6):679–82. Available from: https://doi.org/10.1016/j.cap.2019.03.017
50. Hovgaard MB, Dong M, Otzen DE, Besenbacher F. Quartz Crystal Microbalance Studies of Multilayer Glucagon Fibrillation at the Solid-Liquid Interface. Biophysical Journal [Internet]. 2007 May 19;93(6):2162–9. Available from: https://doi.org/10.1529/biophysj.107.109686
51. Ren D, Shen X, Li C, Cao X. The fractional Kelvin-Voigt model for Rayleigh surface waves in viscoelastic FGM infinite half space. Mechanics Research Communications [Internet]. 2017 Dec 29;87:53–8. Available from: https://doi.org/10.1016/j.mechrescom.2017.12.004
52. Lagarias JC, Reeds JA, Wright MH, Wright PE. Convergence Properties of the Nelder--Mead Simplex Method in Low Dimensions. SIAM Journal on Optimization [Internet]. 1998 Jan 1;9(1):112–47. Available from: https://doi.org/10.1137/s1052623496303470
53. Kasper M, Traxler L, Salopek J, Grabmayr H, Ebner A, Kienberger F. Broadband 120 MHz Impedance Quartz Crystal Microbalance (QCM) with Calibrated Resistance and Quantitative Dissipation for Biosensing Measurements at Higher Harmonic Frequencies. Biosensors [Internet]. 2016 May 25;6(2):23. Available from: https://doi.org/10.3390/bios6020023
54. Ganesan A, Rajendran G, Ercole A, Seshia A. Multifrequency acoustics as a probe of mesoscopic blood coagulation dynamics. Applied Physics Letters [Internet]. 2016 Aug 8;109(6). Available from: https://doi.org/10.1063/1.4960978
55. Guthold M, Liu W, Sparks EA, Jawerth LM, Peng L, Falvo M, et al. A Comparison of the Mechanical and Structural Properties of Fibrin Fibers with Other Protein Fibers. Cell Biochemistry and Biophysics [Internet]. 2007 Oct 1;49(3):165–81. Available from: https://doi.org/10.1007/s12013-007-9001-4
56. Litvinov RI, Weisel JW. Fibrin mechanical properties and their structural origins. Matrix Biology [Internet]. 2016 Aug 23;60–61:110–23. Available from: https://doi.org/10.1016/j.matbio.2016.08.003
57. Ramanujam RK, Maksudov F, Litvinov RI, Nagaswami C, Weisel JW, Tutwiler V, et al. Biomechanics, Energetics, and Structural Basis of Rupture of Fibrin Networks. Advanced Healthcare Materials [Internet]. 2023 Aug 23;12(27). Available from: https://doi.org/10.1002/adhm.202300096
58. GraphPad Prism version 5.0.0 for Windows, GraphPad Software, Boston, Massachusetts USA, www.graphpad.com".

# 8 CURRICULUM VITAE